

A New Nurse Frog (Allobates, Aromobatidae) with a Cricket-Like Advertisement Call from Eastern Amazonia

Authors: Moraes, Leandro J.C.L., and Lima, Albertina P.

Source: *Herpetologica*, 77(2) : 146-163

Published By: The Herpetologists' League

URL: <https://doi.org/10.1655/Herpetologica-D-20-00010.1>

BioOne Complete (complete.BioOne.org) is a full-text database of 200 subscribed and open-access titles in the biological, ecological, and environmental sciences published by nonprofit societies, associations, museums, institutions, and presses.

Your use of this PDF, the BioOne Complete website, and all posted and associated content indicates your acceptance of BioOne's Terms of Use, available at www.bioone.org/terms-of-use.

Usage of BioOne Complete content is strictly limited to personal, educational, and non - commercial use. Commercial inquiries or rights and permissions requests should be directed to the individual publisher as copyright holder.

BioOne sees sustainable scholarly publishing as an inherently collaborative enterprise connecting authors, nonprofit publishers, academic institutions, research libraries, and research funders in the common goal of maximizing access to critical research.

A New Nurse Frog (*Allobates*, Aromobatidae) with a Cricket-like Advertisement Call from Eastern Amazonia

LEANDRO J.C.L. MORAES¹ AND ALBERTINA P. LIMA

Coordenação de Biodiversidade (COBIO), Instituto Nacional de Pesquisas da Amazônia (INPA), Avenida André Araújo 2936, 69067-375, Manaus, Amazonas, Brazil

ABSTRACT: Integrative analyses, long-term studies, and access to remote areas in Amazonia have led to new hypotheses and increased resolution of the systematics and taxonomy of the small nurse frog genus *Allobates* (family Aromobatidae). During anuran sampling in the Middle Tapajós River region, state of Pará, Brazil, we collected data on a new cryptically colored species of *Allobates* with a cricket-like advertisement call. Here, we name and describe this new species, following an integration of phenotypic, ecological, and molecular analyses. The results of a phylogenetic analysis based on mitochondrial and nuclear DNA placed the new species as the sister taxon of *Allobates grillisimilis*. Genetic *p*-distances between the two sister taxa at the 16S region of the mitochondrial DNA ranged from 7% to 9%. A sister-species relationship between the new species and *A. grillisimilis* is also supported by phenotypic evidence. Adults of the new species are small (snout–vent length 15.2–16.8 mm in males and 16.5–17.7 mm in females), with a dorsum uniformly tan to reddish brown, a dark brown lateral stripe and a white ventrolateral stripe, arms pale tan brown and legs greyish-brown, and venter yellowish colored, with variable extension and shades of yellow, paler on the throat. The advertisement call is a trill with a mean peak frequency of 5830.2 Hz, arranged in series of short, closely spaced, pulses (mean of 24.3 pulses/s), and followed by silent intervals of variable duration. We discuss the putative drivers generating and maintaining the distinctiveness between the new species and the allopatrically distributed sister taxon, and on threats to the persistence of the new species. With this species description, the Middle Tapajós River region is consolidated as having one of the highest alpha diversities for the genus *Allobates* in Amazonia.

Key words: Anura; Bioacoustics; Biogeography; Brazil; Conservation; Cryptic diversity; DNA; Integrative taxonomy; Pará

KNOWLEDGE of the systematics and taxonomy of Amazonian amphibians has increased dramatically in recent decades (e.g., Caminer and Ron 2014; Ferrão et al. 2016, 2019; Vacher et al. 2017; Jaramillo et al. 2020). Such increase can be directly attributed to filling of knowledge gaps through the increased integration of multiple and more robust statistical analyses, and data from distinct evolutionary sources, especially molecular evidence (Padial et al. 2010; Simões et al. 2013a). This knowledge advance is also the result of the continuous exploration of new areas and increased sampling effort, reaching historically difficult-to-access localities within the vast geographic range of Amazonia (Moraes et al. 2017, 2019; Simões et al. 2018), as well as long-term inventories (Ferrão et al. 2016; Moraes et al. 2016, 2019). Regarding frogs, new hypotheses and decision-making on the systematics and taxonomy of the aromobatid genus *Allobates* has benefited greatly from this growth in knowledge (Melo-Sampaio et al. 2018; Lima et al. 2020). Ultimately, the increased resolution resulting from incorporation of molecular data in integrative taxonomy approaches, especially mitochondrial DNA, has made this a necessary standard for discovering species diversity within this genus (e.g., Simões et al. 2010, 2019; Souza et al. 2020).

Members of the genus *Allobates* are small diurnal terrestrial frogs (Grant et al. 2006). They are important components of the anuran communities of Neotropical forests, especially in Amazonia, which has the greatest diversity of the genus (Grant et al. 2006, 2017; Frost 2019). This genus currently contains 57 species, but there are indications that the true diversity remains severely underestimated (Grant et al. 2017; Réjaud et al. 2020). Knowledge of phylogenetic relationships among species in this genus is also increasing, with a recent taxonomic revision of Aromobatidae

based on phenotypic and molecular data recognizing four major clades within *Allobates*: two cis-Andean Amazonian, one trans-Andean and one from the Atlantic Forest (Grant et al. 2017). These four major clades were also recovered by the most recent large-scale molecular phylogenetic inference for *Allobates*, which further segregated the genus into nine subclades and investigated their biogeographic history (Réjaud et al. 2020). Despite these advances, the resolution of phylogenetic relationships, systematics, and taxonomy of *Allobates* provide an interesting series of challenges for the years ahead. Increased resolution of these issues will be the result of the continuous effort to (1) integrate genomic-scale data into phylogenies (e.g., Réjaud et al. 2020), (2) describe new species and split species complexes (e.g., Lima et al. 2020), (3) acquire molecular data for species only supported by phenotypic data or re-analyze their type material (e.g., Melo-Sampaio et al. 2020), and (4) formally describe the major subclades sensu Grant et al. (2017) and Réjaud et al. (2020).

The Tapajós River basin (TRB) is drained by one of the largest tributaries in the southern part of the Amazon River and is located entirely within Brazilian territory (Moraes et al. 2020). Although the TRB harbors species-rich regional biotas from a variety of taxa (Moraes et al. 2016; Oliveira et al. 2016), the local diversity of the genus *Allobates* was, until recently, underrecognized (Lima et al. 2014). The description of four new species inhabiting the TRB in the past two decades, and the extension of geographic distributions (Morales 2002; Lima et al. 2014, 2015; Moraes et al. 2019), have shown that some localities within the TRB can hold up to six sympatric *Allobates*, which is considered a high level of local-richness for the genus (see Réjaud et al. 2020). Such high diversity may be a result of the broad environmental heterogeneity and dynamic landscape history of the TRB, which combines the influence of distinct forest types,

¹ CORRESPONDENCE: e-mail, leandro.jclm@gmail.com

geologic basements, and climatic zones (Moraes et al. 2016, 2020). Such features mean the TRB is particularly relevant for studies involving the diversity, biogeography, and evolution of *Allobates* because it is a geographic focal point for the discovery of new species within this genus.

During recent anuran surveys in the TRB, we collected data pertaining to a cryptically colored *Allobates* with a cricket-like advertisement call on the east bank of the Middle Tapajós River region. After careful analysis of this newly collected material, considering morphological, acoustic, ecological, and molecular evidences, we conclude that it represents an undescribed species. Here, we name and describe this new species using an integrative approach, and investigate its phylogenetic relationships on the basis of the molecular variation.

MATERIALS AND METHODS

Specimens and natural history data for the new species of *Allobates* were collected by A.P. Lima during field expeditions in 2018 and 2019 to the Middle Tapajós River region, state of Pará, Brazil. Adult individuals were euthanized with a topical solution of 2% lidocaine, fixed with 10% formalin for 24 h, and preserved in 70% ethanol. Tadpoles were collected from egg-masses, raised to three developmental stages (27, 29, and 31) following the categories described by Gosner (1960), euthanized in a dilute solution of benzocaine, and preserved in 10% formalin. For molecular analyses, muscle tissues were obtained before fixing and preserving specimens and stored in 100% ethanol. Color patterns of living specimens were described using photographs and field notes. Specimens were deposited in the Herpetological Collection of the Museu Paraense Emílio Goeldi, Belém, Pará, Brazil (MPEG) and the Collection of Amphibians and Reptiles (INPA-H) of the Instituto Nacional de Pesquisas da Amazônia (INPA), Manaus, Amazonas, Brazil. The taxonomic status of the newly collected material was investigated with an integrative approach (Padial et al. 2010), through the combined analyses of morphological, acoustic, molecular, and ecological data. We compared the external morphology of adults and tadpoles of the new species with published information on *Allobates*, as well as through direct examination of voucher specimens of 25 species housed at the INPA-H, including type material (Appendix). We restricted our phenotypic comparisons for the new species description to seven congeners, using two combined filters: (1) syntopic or geographically close species, *A. crombiei* (Morales 2002), *A. femoralis* (Boulenger 1884), *A. magnussoni* Lima, Simões and Kaefer 2014, *A. nunciatus* Moraes, Pavan and Lima 2019 and *A. tapajós* Lima, Simões and Kaefer 2015, based on the fact that the known geographic distribution of the new species is restricted to eastern Amazonia, south of the Amazon River (Brazilian Shield), approximately 700 km from the nearest country border, and widely distributed species of *Allobates* are rare or involve undetected cryptic species complexes (see Lima et al. 2020); and, (2) closely related congeners of the same major clade, *A. caeruleodactylus* (Lima and Caldwell 2001) and *A. grillisimilis* Simões, Sturaro, Peloso and Lima 2013, based on molecular similarities of the new species within a most inclusive and best supported monophyletic species group.

Adult external morphology of the new species was evaluated using 21 specimens. Morphological terminology followed Grant et al. (2006), and measurements followed Lima et al. (2007). Sex was determined from calling activity and/or the presence of vocal slits in males. The following 23 measurements were taken from specimens under a stereomicroscope with graduated lenses (to the nearest 0.01 mm): snout–vent length (SVL); head width, at level of angle of jaw (HW); head length, from angle of jaw to tip of snout (HL); snout length, from proximal edge of eye to tip of snout (SL); interorbital distance (IO); internarial distance (IN); eye diameter (ED); eye–nostril distance (EN); tympanum diameter (TD); forearm length, from edge of hand to the outer edge of flexed elbow (FA); upper arm length, from insertion at body to outer edge of flexed elbow (UA); hand lengths, from proximal edge of palmar tubercle to tips of fingers I, II, III, and IV (respectively HAND I, HAND II, HAND III, HAND IV); thigh length, from the posterior extremity of the urostyle to the knee (TH); tibia length, from proximal edge of flexed knee to heel (TL); foot length, from proximal edge of outer metatarsal tubercle to the tip of Toe IV (FL); width of Finger III disc (WFD); width of palmar tubercle (WPT); width of thenar tubercle (WTT); width of the third phalanx of Finger III (WPF); width of Toe IV disc (WTD). Measurements were summarized as mean \pm standard deviation and range. Fingers and toes were numbered preaxially to postaxially from I–IV and I–V, respectively. The toe webbing formula followed Savage and Heyer (1997). Color photographs of the new species are freely available at the Sapoteca project website (see <http://ppbio.inpa.gov.br/en/sapoteca/home>).

Eighteen tadpole specimens were used for the larvae description. Morphological terminology, measurements, and diagnostic characters followed Altig and McDiarmid (1999). Tadpoles were grouped according to their developmental stage (Gosner 1960). For each group, the following measurements were taken under a stereomicroscope with graduated lenses (to the nearest 0.01 mm): total length, from tip of snout to tip of tail (TOL); body length, from tip of snout to body–tail insertion (BL); tail length, from body–tail insertion to tip of tail (TAL); body width at level of spiracle (BW); body height at level of spiracle (BH); head width at level of eyes (HW); tail maximum height (TH); tail muscle maximum height (TMH); tail muscle maximum width (TMW); interorbital distance (IO); internarial distance (IN); eye–nostril distance (EN); naris–snout distance (NS); spiracle–snout distance (SS); eye diameter (ED); vent tube length (VTL); spiracle tube length (STL); oral disc width (OD); posterior labium width (PL); anterior labium width (AL); upper jaw sheath length (UJL); upper jaw sheath width (UJW); length of first anterior tooth row (A1); length of second anterior tooth row (A2); length of median gap in second anterior tooth row 2 (GAP); length of first posterior tooth row (P1); length of second posterior tooth row (P2); length of third posterior tooth row (P3). Measurements were summarized as mean \pm standard deviation and range.

Advertisement calls of males of the new species were recorded about 1–2 m from the emitter with a SONY PCM-D50 Digital Audio Recorder at a sampling frequency of 44 kHz and 16-bit resolution and stored in uncompressed WAV format ($n = 11$ recordings). Air temperature during recordings varied between 24.8° and 27.0°C. Footage of one

calling male is also freely available at the Sapoteca project website. Call structure is composed of a variable number of short pulses sometimes slightly different in temporal and spectral parameters, and we independently measured the parameters from the first, central, and last pulses. Parameters selected for measurement are considered standard in anuran and dendrobatoid taxonomy (Santos et al. 2014; Köhler et al. 2017) and were used for the description of the sister taxon *A. grillisimilis*. Temporal parameters included the number of pulses per call (PPC); intercall interval (ICI); interpulse interval between first and second pulse (IPF); interpulse interval between central and subsequent pulse (IPC); call duration (CAD); first pulse duration (FPD); central pulse duration (CPD); last pulse duration (LPD); and pulse emission rate (PER). Spectral parameters include lowest, peak, and highest frequencies for the whole call (LFC, PFC, HFC), first pulses (LFF, PFF, HFF), central pulses (LCE, PCE, HCE), and last pulses (LFL, PFL, HFL). These data were measured for up to five calls of each recording, summarized as mean \pm standard deviation and range, and compared with other *Allobates* calls described in the literature and original recordings from the description of the sister taxon *A. grillisimilis*. We conducted the acoustic analyses in Raven Pro (v1.5; Cornell Laboratory of Ornithology, Ithaca, NY), and generated graphic representations in Program R environment (v3.6.1; R Core Team 2019), using the packages seewave (v2.1.4; Sueur et al. 2008) and TuneR (v1.3.3; Ligges et al. 2018). Detailed information on the recordings of the new species and *A. grillisimilis* included in acoustic analyses can be found in Supplemental Material Table S1, available online.

For the molecular-based phylogenetic analysis, we compiled a database with information of eight genetic markers, downloaded from the online repository GenBank. Four of these genes are from mitochondrial DNA (mtDNA): the 12S and 16S ribosomal RNA (rRNA) genes, and the protein-coding genes (CDS) cytochrome oxidase I (COI), and cytochrome b (CYTB). The other four genes are CDS from nuclear DNA (nuDNA): histone H3 (HH3), recombination activating gene 1 (RAG1), rhodopsin (RHO), and seventh in absentia (SINA). We did not download other available genetic markers because they are not minimally representative considering our data set and would have increased the volume of missing data. Taxon sampling includes representative samples for nominal and candidate species of *Allobates* with available molecular data, as well as all available samples of the sister taxon *A. grillisimilis* and the closely related species *A. caeruleodactylus*. Representatives of four related genera were included as outgroups: *Anomaloglossus stephensi* (Martins 1989), *Aromobates nocturnus* Myers, Paolillo and Daly 1991, *Mannophryne collaris* (Boulenger 1912) and *Rheobates palmatus* (Werner 1899). To position the new species in this database, we generated 16S sequences for five adult and two larval specimens. We focused on this gene because it is considered a comprehensive genetic marker for decision-making in both the taxonomy of amphibians (Vences et al. 2012; Lyra et al. 2017) as well as the genus *Allobates* (see Simões et al. 2013a,b, 2018, 2019; Lima et al. 2014, 2015; Simões 2016).

Genomic DNA was extracted using standard protocols for a commercial kit (Wizard® Genomic DNA Purification Kit, Promega Corp.), with the target fragment amplified via

Polymerase Chain Reaction (PCR), using the primers 16Sar/16Sbr (Palumbi et al. 1991) and standard protocols (see Simões 2016). PCR products were purified with polyethyleneglycol (PEG) 8000 and sequenced using standard protocols of the Big Dye™ Terminator Kit (Applied Biosystems) in an ABI PRISM® 3500 (Applied Biosystems) automated sequencer. We used Geneious (v6; Biomatters, Auckland, New Zealand; Kearse et al. 2012) to edit the raw sequences, and deposited them in GenBank. The complete information related to these sequences, and the others included in molecular analyses, can be found in Supplemental Material Table S2, available online.

Each gene was independently aligned using the MAFFT online server with default parameters, except for the use of E-INS-i strategy for RNAs and G-INS-i strategy for CDS (Katoh and Standley 2013). The genes were posteriorly concatenated, reaching a final alignment with 77 terminals (73 *Allobates* + 4 outgroups) and 5028 base pairs (bp). Using this alignment, we performed a phylogenetic inference under a Bayesian framework with MrBayes (v3.2.6; Ronquist et al. 2012). We initially divided the data set into 19 partitions (one for each codon position of the CDS and one for the RNAs) and determined the models of nucleotide evolution and best-fit partition schemes under the Bayesian Information Criterion (BIC) using PartitionFinder (v2.1.1; Lanfear et al. 2017). We conducted the analysis with two parallel runs of Markov chain Monte Carlo chains with 100 million iterations, with 10,000 thinning and 10% initial burn-in. Convergence of parameters (standard deviation of split frequencies <0.01 and estimated sample size >200) were assessed using Tracer (v1.7; Rambaut et al. 2018), and the maximum clade credibility tree was extracted. Using the most representative gene in our sampling (16S, all individuals, 543 bp), we used MEGA (v7; Kumar et al. 2016) to compute the uncorrected pairwise genetic distances between the samples, with gaps removed using a pairwise deletion option.

RESULTS

Phylogenetic Relationships and Genetic Distances

Our molecular phylogenetic analysis based on concatenated data set of eight genes (four mtDNA and four nuDNA) compared the newly collected samples from the Middle Tapajós River region with 41 nominal species of *Allobates*, representing a large portion (72%) of the currently known diversity of the genus (57 species), as well as another 17 candidate species (Fig. 1). The tree topology supports the monophyly of *Allobates* with high nodal support. Initial divergence within this genus is related to the split of the Atlantic Forest species *A. olfersioides* (Lutz 1925) and a major clade containing trans- and cis-Andean species. Early divergent species within this major clade are distributed at the western Guiana Shield in northern Amazonia: *A. undulatus* (Myers and Donnelly 2001) and one unnamed species (*A. sp.* “Neblina”). The subsequent divergence split the trans-Andean group and an ingroup formed by the remaining species of the cis-Andean Amazonia set. Interrelationships among some of the cis-Andean ingroup clades (sensu Réjaud et al. 2020) received lower nodal supports, especially the *A. femoralis* clade, *A. kingsburyi* clade, *A. trilineatus* clade, and *A. caeruleodactylus* clade, with the

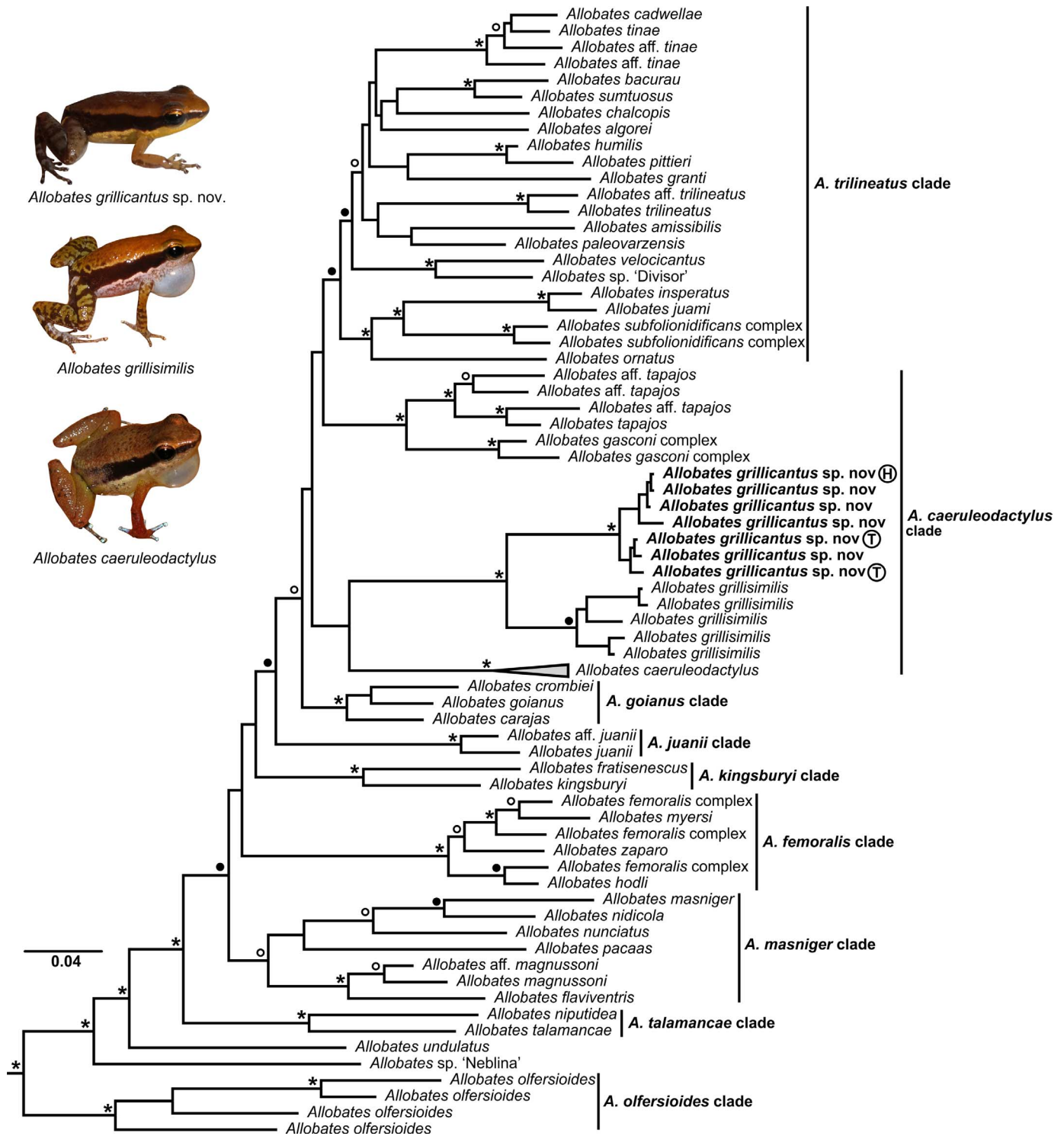


FIG. 1.—Bayesian phylogenetic tree of *Allobates* inferred from a concatenated data set of eight genes (four mitochondrial and four nuclear), highlighting the position of the new species from the Middle Tapajós River region, state of Pará, Brazil as the sister taxon of *Allobates grillisimilis*. Outgroups were omitted, and the informal clade names to right of the tree follow the subdivision of Réjaud et al. (2020). Support values are shown above branches: asterisks represent posterior probability 1.00–0.99, black circles 0.98–0.95, open circles 0.94–0.85, and support below this level were omitted. (H) Holotype; (T) Tadpole. Photographs by A.P. Lima. A color version of this figure is available online.

latter being split in two subclades (Fig. 1). The newly collected samples from the Middle Tapajós River region clustered together and were positioned as a member of this major cis-Andean ingroup, with high nodal supports (Fig. 1). At a finer scale, the cluster of newly collected samples was

highly supported as the sister taxon of *A. grillisimilis* (Fig. 1), as expected given the phenotypic similarities between these taxa.

Minimum mean genetic distances between species pairs of analyzed *Allobates* occurred between *A. humilis* (Rivero

TABLE 1.—Measurements (in mm) of the type series of *Allobates grillicantus*, from the Middle Tapajós River region, state of Pará, Brazil, highlighting the data of the holotype (MPEG 43046, adult male). Values represent mean \pm standard deviation, with range shown in parentheses. See text for measurements acronyms.

Measurements	Holotype (male)	Males (n = 13)	Females (n = 5)
SVL	16.40	15.80 \pm 0.52 (15.20–16.80)	17.16 \pm 0.58 (16.50–17.70)
HW	5.50	5.26 \pm 0.21 (4.90–5.70)	5.70 \pm 0.16 (5.50–5.90)
HL	5.60	5.00 \pm 0.28 (4.70–5.60)	5.24 \pm 0.36 (4.60–5.50)
SL	2.25	2.34 \pm 0.13 (2.10–2.50)	2.47 \pm 0.22 (2.15–2.75)
EN	1.50	1.55 \pm 0.05 (1.50–1.65)	1.68 \pm 0.07 (1.55–1.75)
ED	2.60	2.37 \pm 0.12 (2.20–2.60)	2.54 \pm 0.14 (2.40–2.75)
IO	4.60	4.70 \pm 0.16 (4.40–5.00)	4.86 \pm 0.05 (4.80–4.90)
IN	2.20	2.22 \pm 0.09 (2.00–2.40)	2.50 \pm 0.40 (2.20–3.20)
TYM	1.05	1.04 \pm 0.06 (0.95–1.15)	1.11 \pm 0.09 (1.00–1.25)
UA	4.10	4.13 \pm 0.16 (4.00–4.50)	4.06 \pm 0.35 (3.50–4.40)
FA	3.70	3.29 \pm 0.25 (2.80–3.70)	3.18 \pm 0.39 (2.50–3.50)
HAND 1	3.05	3.19 \pm 0.29 (2.75–3.75)	3.36 \pm 0.14 (3.20–3.55)
HAND 2	2.90	2.90 \pm 0.22 (2.45–3.35)	3.03 \pm 0.07 (2.95–3.15)
HAND 3	4.10	4.07 \pm 0.16 (3.75–4.40)	4.20 \pm 0.17 (4.00–4.45)
HAND 4	2.65	2.58 \pm 0.16 (2.25–2.80)	2.76 \pm 0.11 (2.60–2.90)
TH	7.60	7.05 \pm 0.53 (6.10–7.90)	7.30 \pm 0.20 (7.00–7.50)
TL	8.20	7.60 \pm 0.40 (7.00–8.20)	7.76 \pm 0.13 (7.70–8.00)
FL	7.10	6.79 \pm 0.35 (6.00–7.40)	7.10 \pm 0.30 (6.60–7.40)
WFD	0.60	0.61 \pm 0.06 (0.50–0.70)	0.64 \pm 0.11 (0.50–0.75)
WPF	0.40	0.42 \pm 0.03 (0.35–0.45)	0.42 \pm 0.06 (0.35–0.50)
WPT	0.50	0.54 \pm 0.07 (0.50–0.70)	0.59 \pm 0.07 (0.50–0.70)
WTT	0.25	0.30 \pm 0.06 (0.25–0.40)	0.31 \pm 0.07 (0.20–0.40)
WTD	0.85	0.74 \pm 0.11 (0.55–0.85)	0.78 \pm 0.11 (0.60–0.85)

1980) vs. *A. pittieri* (La Marca, Manzanilla, and Mijares-Urrutia 2004; 2.9%); *A. juami* Simões, Gagliardi-Urrutia, Rojas-Runjaic and Castroviejo-Fisher, 2018 vs. *A. insperatus* (Morales 2002; 2.9%); *A. femoralis* vs. *A. hodli* Simões, Lima and Farias 2010 (3.4%); and *A. tinae* Melo-Sampaio, Oliveira and Prates 2018 vs. *A. caldwella* Lima, Ferrão and Silva 2020 (3.4%). In some cases, the mean genetic distances between the samples of a nominal species surpassed the interspecific 2.9% threshold, indicating a putative case of cryptic diversity. This was the case in *A. grillisimilis* (3.0%), *A. femoralis* (3.3%), *A. gasconi* (Morales 2002; 3.6%), *A. juanii* (Morales 1994; 3.6%), *A. tinae-caldwellae* (4.3%), *A. tapajos* (5.5%), and *A. olfersioides* (9.6%). Uncorrected pairwise genetic distances between the newly collected samples and the most closely related species (*A. grillisimilis*) ranged from 6.7% to 9.6%, and from 9.5% to 18.2% compared with remaining *Allobates* included in the analysis. Therefore, the monophyly, the tree topology, and genetic distinctiveness of these newly collected samples clearly show that they are representatives of an unnamed species, which we describe below.

SPECIES DESCRIPTION

Allobates grillicantus sp. nov.
(Tables 1–3; Figs. 2–8, 10)

Holotype.—Adult male (MPEG 43046, field number APL 22394, 16.4 mm SVL; Figs. 2–4, 7) collected by A.P. Lima on 20 February 2019, on the east bank of Middle Tapajós River, municipality of Trairão, state of Pará, Brazil (04°45'25.1"S, 55°57'56.4"W; datum = WGS84 in all cases).

Paratopotypes.—Twelve adult specimens, 9 males (MPEG 43038–43041, 43045, 43047–43050) and 3 females (MPEG 43042–43044); 28 larval specimens (lots MPEG 43051–43053); all collected by A.P. Lima between 11–20 February 2019.

Paratypes.—Five adult specimens, 3 males (INPA-H 41352–41353, 41356) and 2 females (INPA-H 41354–41355); 13 larval specimens (lot INPA-H 41357); all collected by A.P. Lima on 13 February 2019 at km 24 of the Brazilian federal highway BR-163, east bank of Middle Tapajós River, municipality of Trairão, state of Pará, Brazil (04°52'53.7"S, 56°09'44.4"W).

Etymology.—The specific epithet *grillicantus* means “cricket song” and refers to the cricket-like advertisement call emitted by this species. It is a compound Latin noun in the nominative case used in apposition, derived from *gryllus*, meaning “cricket” and *cantus*, meaning “song.” The name is purposely similar to the sister taxon *A. grillisimilis* to refer to common ancestry.

Generic placement.—The new species is placed in the genus *Allobates* based on phenotypic similarities to the other species of this genus and on the results of the molecular-based phylogenetic analysis.

Diagnosis.—A small species of cryptically colored *Allobates*, characterized by mean SVL of adult males 15.8 mm (range = 15.2–16.8 mm; $n = 13$; Table 1), adult females 17.2 mm (range = 16.5–17.7 mm; $n = 5$; Table 1); skin texture of dorsum smooth to shagreened, in some specimens with scattered granules, more prominent posteriorly; Finger II slightly shorter than Finger I; Finger III of adult males with weakly developed preaxial swelling with uniform width, but not measurably wider than Finger III of adult females; distal subarticular tubercle absent on Finger IV; palmar tubercle drop-shaped; finger and toe discs expanded, most prominent in toes II, III, and IV; absence of lateral fringes on fingers and toes; basal webbing present between toes III and IV, webbing formula III 2^{1/2}–3^{1/2} IV; tympanum conspicuous, small; vocal sac distinct, single and subgular; dorsum uniformly tan to reddish brown with no distinct contrasting marks, dark brown in preservative; pale dorso-lateral stripe absent in life, but present in preservative;

TABLE 2.—Advertisement call parameters of *Allobates grillicantus*, from the Middle Tapajós River region, state of Pará, Brazil, compared with parameters from distinct populations of its sister taxon *Allobates grillisimilis*. Parameters are based on field recordings of calling males ($n = 11$ recordings for *A. grillicantus*) and literature data. Parameters are given as mean \pm standard deviation, with range shown in parentheses. See text for definition of acronyms and Supplemental Material Table S1 (available online) for additional details on the recordings.

Measurements	<i>A. grillicantus</i>		<i>A. grillisimilis</i> (Borba)		<i>A. grillisimilis</i> (Nova Olinda)		<i>A. grillisimilis</i> (Matiés)	
	3–15	3–10	3–10	3–15	3–15	3–6	3–6	5
PPC (range)	3–15	3–10	3–10	3–15	3–15	3–6	3–6	5
PPC (mode)	4	5	5	4	4	5	5	5
ICI (s)	0.865 \pm 0.317 (0.411–1.677)	1.525 \pm 0.312 (0.920–1.999)	0.865 \pm 0.312 (0.920–1.999)	0.912 \pm 0.299 (0.695–1.347)	0.912 \pm 0.299 (0.695–1.347)	1.192 \pm 0.248 (0.899–1.403)	1.192 \pm 0.248 (0.899–1.403)	1.192 \pm 0.248 (0.899–1.403)
IPF (s)	0.020 \pm 0.003 (0.013–0.027)	0.014 \pm 0.002 (0.010–0.020)	0.014 \pm 0.002 (0.010–0.020)	0.020 \pm 0.002 (0.017–0.023)	0.020 \pm 0.002 (0.017–0.023)	0.020 \pm 0.003 (0.015–0.020)	0.020 \pm 0.003 (0.015–0.020)	0.020 \pm 0.003 (0.015–0.020)
IPC (s)	0.025 \pm 0.004 (0.015–0.033)	0.017 \pm 0.002 (0.013–0.019)	0.017 \pm 0.002 (0.013–0.019)	0.023 \pm 0.003 (0.020–0.027)	0.023 \pm 0.003 (0.020–0.027)	0.026 \pm 0.012 (0.018–0.043)	0.026 \pm 0.012 (0.018–0.043)	0.026 \pm 0.012 (0.018–0.043)
CAD (s)	0.264 \pm 0.073 (0.151–0.507)	0.178 \pm 0.035 (0.122–0.244)	0.178 \pm 0.035 (0.122–0.244)	0.227 \pm 0.053 (0.170–0.305)	0.227 \pm 0.053 (0.170–0.305)	0.149 \pm 0.011 (0.141–0.165)	0.149 \pm 0.011 (0.141–0.165)	0.149 \pm 0.011 (0.141–0.165)
FPP (s)	0.021 \pm 0.003 (0.016–0.030)	0.022 \pm 0.006 (0.016–0.030)	0.022 \pm 0.006 (0.016–0.030)	0.015 \pm 0.003 (0.012–0.020)	0.015 \pm 0.003 (0.012–0.020)	0.016 \pm 0.003 (0.013–0.021)	0.016 \pm 0.003 (0.013–0.021)	0.016 \pm 0.003 (0.013–0.021)
CPD (s)	0.021 \pm 0.005 (0.014–0.034)	0.019 \pm 0.004 (0.012–0.024)	0.019 \pm 0.004 (0.012–0.024)	0.017 \pm 0.002 (0.013–0.020)	0.017 \pm 0.002 (0.013–0.020)	0.017 \pm 0.002 (0.015–0.019)	0.017 \pm 0.002 (0.015–0.019)	0.017 \pm 0.002 (0.015–0.019)
LPD (s)	0.021 \pm 0.007 (0.012–0.037)	0.019 \pm 0.004 (0.013–0.023)	0.019 \pm 0.004 (0.013–0.023)	0.016 \pm 0.003 (0.012–0.020)	0.016 \pm 0.003 (0.012–0.020)	0.016 \pm 0.002 (0.014–0.019)	0.016 \pm 0.002 (0.014–0.019)	0.016 \pm 0.002 (0.014–0.019)
LFC (Hz)	5137.6 \pm 312.9 (4470.9–5676.6)	5690.4 \pm 142.8 (5518.8–5913.3)	5690.4 \pm 142.8 (5518.8–5913.3)	5609.4 \pm 106.5 (5446.1–5738.7)	5609.4 \pm 106.5 (5446.1–5738.7)	5282.8 \pm 178.3 (5056.6–5437.6)	5282.8 \pm 178.3 (5056.6–5437.6)	5282.8 \pm 178.3 (5056.6–5437.6)
PFC (Hz)	5830.2 \pm 231.4 (5512.5–6373.8)	6394.2 \pm 169.4 (6200.2–6651.0)	6394.2 \pm 169.4 (6200.2–6651.0)	6219.9 \pm 153.9 (6011.7–6363.2)	6219.9 \pm 153.9 (6011.7–6363.2)	5964.7 \pm 96.3 (5867.8–6061.6)	5964.7 \pm 96.3 (5867.8–6061.6)	5964.7 \pm 96.3 (5867.8–6061.6)
HFC (Hz)	6267.0 \pm 217.0 (5981.9–6707.5)	6906.2 \pm 217.4 (6654.8–7414.9)	6906.2 \pm 217.4 (6654.8–7414.9)	6631.3 \pm 165.5 (6411.7–6797.6)	6631.3 \pm 165.5 (6411.7–6797.6)	6906.2 \pm 217.4 (6654.8–7414.9)	6906.2 \pm 217.4 (6654.8–7414.9)	6906.2 \pm 217.4 (6654.8–7414.9)
LFF (Hz)	5168.8 \pm 317.3 (4423.4–5690.7)	5664.7 \pm 158.2 (5494.7–5908.3)	5664.7 \pm 158.2 (5494.7–5908.3)	5559.3 \pm 102.5 (5405.5–5698.6)	5559.3 \pm 102.5 (5405.5–5698.6)	5283.0 \pm 161.6 (5085.7–5427.3)	5283.0 \pm 161.6 (5085.7–5427.3)	5283.0 \pm 161.6 (5085.7–5427.3)
FFF (Hz)	5817.3 \pm 218.2 (5340.2–6201.6)	6230.2 \pm 185.3 (5881.2–6488.2)	6230.2 \pm 185.3 (5881.2–6488.2)	6016.3 \pm 108.9 (5834.9–6127.9)	6016.3 \pm 108.9 (5834.9–6127.9)	5815.3 \pm 111.0 (5671.3–5902.8)	5815.3 \pm 111.0 (5671.3–5902.8)	5815.3 \pm 111.0 (5671.3–5902.8)
HFF (Hz)	6194.0 \pm 212.6 (5894.6–6606.3)	6774.2 \pm 295.9 (6450.3–7430.0)	6774.2 \pm 295.9 (6450.3–7430.0)	6374.0 \pm 79.6 (6237.6–6449.4)	6374.0 \pm 79.6 (6237.6–6449.4)	6178.6 \pm 153.4 (5982.3–6318.1)	6178.6 \pm 153.4 (5982.3–6318.1)	6178.6 \pm 153.4 (5982.3–6318.1)
LCE (Hz)	5328.4 \pm 314.0 (4595.5–5780.4)	5900.1 \pm 164.3 (5642.2–6108.9)	5900.1 \pm 164.3 (5642.2–6108.9)	5781.9 \pm 173.2 (5538.5–5951.3)	5781.9 \pm 173.2 (5538.5–5951.3)	5507.6 \pm 164.2 (5298.1–5698.2)	5507.6 \pm 164.2 (5298.1–5698.2)	5507.6 \pm 164.2 (5298.1–5698.2)
PCE (Hz)	5843.5 \pm 228.3 (5437.5–6373.8)	6434.9 \pm 161.3 (6247.3–6714.3)	6434.9 \pm 161.3 (6247.3–6714.3)	6228.2 \pm 150.6 (6007.8–6360.3)	6228.2 \pm 150.6 (6007.8–6360.3)	6014.5 \pm 90.7 (5924.3–6093.9)	6014.5 \pm 90.7 (5924.3–6093.9)	6014.5 \pm 90.7 (5924.3–6093.9)
HCE (Hz)	6218.6 \pm 235.1 (5860.3–6721.1)	6884.3 \pm 178.2 (6636.6–7207.7)	6884.3 \pm 178.2 (6636.6–7207.7)	6588.8 \pm 130.6 (6400.5–6736.4)	6588.8 \pm 130.6 (6400.5–6736.4)	6358.9 \pm 109.6 (6245.8–6462.2)	6358.9 \pm 109.6 (6245.8–6462.2)	6358.9 \pm 109.6 (6245.8–6462.2)
LFL (Hz)	5336.4 \pm 328.4 (4595.5–5951.4)	5848.8 \pm 159.9 (5570.9–6100.6)	5848.8 \pm 159.9 (5570.9–6100.6)	5788.9 \pm 185.7 (5526.7–5989.7)	5788.9 \pm 185.7 (5526.7–5989.7)	5564.8 \pm 129.9 (5404.2–5720.3)	5564.8 \pm 129.9 (5404.2–5720.3)	5564.8 \pm 129.9 (5404.2–5720.3)
PFL (Hz)	5844.5 \pm 230.6 (5437.5–6373.8)	6359.8 \pm 146.3 (6153.1–6602.6)	6359.8 \pm 146.3 (6153.1–6602.6)	6221.8 \pm 149.7 (6011.7–6343.7)	6221.8 \pm 149.7 (6011.7–6343.7)	6026.6 \pm 97.2 (5929.7–6118.1)	6026.6 \pm 97.2 (5929.7–6118.1)	6026.6 \pm 97.2 (5929.7–6118.1)
HFL (Hz)	6236.0 \pm 230.2 (5902.5–6679.3)	6806.1 \pm 215.7 (6487.8–7206.3)	6806.1 \pm 215.7 (6487.8–7206.3)	6570.4 \pm 138.8 (6404.4–6761.3)	6570.4 \pm 138.8 (6404.4–6761.3)	6365.8 \pm 108.9 (6270.3–6473.9)	6365.8 \pm 108.9 (6270.3–6473.9)	6365.8 \pm 108.9 (6270.3–6473.9)
PER (pulses/s)	24.310 \pm 0.963 (22.123–26.316)	27.585 \pm 0.631 (26.059–28.777)	27.585 \pm 0.631 (26.059–28.777)	26.691 \pm 0.977 (25.078–28.571)	26.691 \pm 0.977 (25.078–28.571)	28.091 \pm 1.220 (26.455–30.075)	28.091 \pm 1.220 (26.455–30.075)	28.091 \pm 1.220 (26.455–30.075)
SVL (mm)	15.7 \pm 0.6 (15.2–16.7) and unvouchered specimens	14.0 \pm 0.6 (13.6–14.9)	14.0 \pm 0.6 (13.6–14.9)	13.0 \pm 0.3 (12.6–13.2)	13.0 \pm 0.3 (12.6–13.2)	Unvouchered specimens	Unvouchered specimens	Unvouchered specimens
Air temperature (°C)	24.8–27.0	24.9–27.9	24.9–27.9	24.2–24.9	24.2–24.9	25.0–26.5	25.0–26.5	25.0–26.5

TABLE 3.—Measurements (in mm) of *Allobates grillicantus* tadpoles from the type locality, on the Middle Tapajós River region, state of Pará, Brazil. Classification in distinct developmental stages followed the categories described by Gosner (1960). Values are given by mean \pm standard deviation, with range shown in parentheses. See text for definitions of acronyms.

Measurements	Stage 27 (n = 5)	Stage 29 (n = 5)	Stage 31 (n = 8)
TOL	15.12 \pm 0.26 (14.70–15.40)	17.80 \pm 1.80 (15.70–19.80)	19.89 \pm 0.56 (19.20–21.00)
BL	4.84 \pm 0.19 (4.60–5.10)	5.88 \pm 0.40 (5.30–6.30)	6.33 \pm 0.26 (5.80–6.60)
TAL	10.28 \pm 0.23 (10.00–10.50)	11.92 \pm 1.45 (10.00–13.50)	13.55 \pm 0.52 (13.00–14.50)
BW	3.28 \pm 0.11 (3.10–3.40)	3.90 \pm 0.38 (3.40–4.40)	4.21 \pm 0.19 (3.90–4.40)
BH	1.88 \pm 0.19 (4.60–5.10)	2.44 \pm 0.09 (2.30–2.50)	2.66 \pm 0.13 (2.50–2.90)
SS	3.32 \pm 0.22 (3.00–3.60)	3.96 \pm 0.19 (3.80–4.30)	3.86 \pm 0.77 (2.00–4.40)
HW	2.82 \pm 0.08 (2.70–2.90)	3.32 \pm 0.16 (3.10–3.50)	3.41 \pm 0.13 (3.20–3.60)
TH	2.24 \pm 0.11 (2.10–2.40)	2.74 \pm 0.20 (2.50–3.00)	3.15 \pm 0.11 (3.00–3.30)
TMW	1.40 \pm 0.00 (1.40–1.40)	1.70 \pm 0.16 (1.50–1.90)	1.89 \pm 0.10 (1.70–2.00)
TMH	1.42 \pm 0.08 (1.30–1.50)	1.68 \pm 0.18 (1.50–1.90)	1.92 \pm 0.07 (1.80–2.00)
IO	1.48 \pm 0.04 (1.40–1.50)	1.68 \pm 0.08 (1.60–1.80)	1.82 \pm 0.05 (1.80–1.90)
IN	1.18 \pm 0.08 (1.10–1.30)	1.10 \pm 0.07 (1.00–1.20)	1.30 \pm 0.05 (1.20–1.40)
EN	0.55 \pm 0.03 (0.50–0.60)	0.78 \pm 0.21 (0.65–1.15)	1.03 \pm 0.28 (0.70–1.35)
NS	0.55 \pm 0.07 (0.45–0.60)	0.62 \pm 0.09 (0.50–0.75)	0.68 \pm 0.07 (0.55–0.75)
ED	0.87 \pm 0.04 (0.80–0.90)	0.96 \pm 0.06 (0.90–1.05)	1.02 \pm 0.03 (1.00–1.10)
VTL	1.16 \pm 0.09 (1.05–1.25)	1.30 \pm 0.21 (1.00–1.50)	1.67 \pm 0.15 (1.40–1.85)
STL	0.45 \pm 0.08 (0.35–0.55)	0.55 \pm 0.05 (0.50–0.60)	0.65 \pm 0.07 (0.50–0.75)
OD	1.44 \pm 0.04 (1.40–1.48)	1.71 \pm 0.24 (1.42–2.00)	1.79 \pm 0.10 (1.64–1.92)
PL	0.33 \pm 0.02 (0.30–0.34)	0.41 \pm 0.04 (0.34–0.46)	0.39 \pm 0.05 (0.30–0.50)
AL	0.42 \pm 0.02 (0.40–0.44)	0.41 \pm 0.04 (0.38–0.48)	0.40 \pm 0.05 (0.34–0.48)
A1	1.15 \pm 0.11 (1.00–1.26)	1.42 \pm 0.19 (1.20–1.66)	1.39 \pm 0.09 (1.24–1.54)
A2	0.38 \pm 0.03 (0.32–0.40)	0.46 \pm 0.07 (0.40–0.56)	0.49 \pm 0.06 (0.40–0.60)
GAP	0.48 \pm 0.02 (0.46–0.52)	0.50 \pm 0.06 (0.42–0.60)	0.48 \pm 0.09 (0.32–0.56)
P1	1.05 \pm 0.12 (1.00–1.12)	1.30 \pm 0.18 (1.16–1.60)	1.27 \pm 0.10 (1.10–1.40)
P2	1.04 \pm 0.12 (0.84–0.92)	1.25 \pm 0.19 (1.08–1.56)	1.28 \pm 0.09 (1.10–1.40)
P3	1.30 \pm 0.08 (1.20–1.40)	0.92 \pm 0.15 (0.74–1.16)	0.94 \pm 0.09 (0.80–1.10)
UJW	0.10 \pm 0.03 (0.06–0.82)	0.12 \pm 0.01 (0.10–0.14)	0.13 \pm 0.03 (0.10–0.18)
UJL	0.78 \pm 0.03 (0.74–0.82)	0.89 \pm 0.14 (0.80–1.14)	0.82 \pm 0.03 (0.80–0.90)

continuous dark brown lateral stripe, from the tip of the snout to the cloacal region; oblique lateral stripe absent; pale whitish ventrolateral stripe present, often diffuse or interrupted; dorsal surface of arms pale brown, cream in preservative; dorsal surface of legs greyish brown, dark brown in preservative; ventral surface yellowish colored in both sexes, with variable extension and shades of yellow, and throat translucent pale yellow, cream in preservative; iris metallic gold to brownish, finely vermiculated; papillae on posterior labium of tadpoles elongate; distinctive advertisement call pattern (see call description section).

Comparisons.—We focused our comparisons on congeners from a subgroup of Amazonian *Allobates* (see Methods; characters of compared species are shown in parentheses). With regards to external morphology, *Allobates grillicantus* is distinguished from the brightly colored *A. femoralis* by a cryptic external coloration at dorsal surfaces, with a color spectrum ranging from brown, ochre, and cream (dorsal surfaces with white dorsolateral stripes on a black background, and bright red, orange, or yellow marks on dorsal surfaces of thighs).

Relative to cryptically colored *Allobates*, *A. grillicantus* is distinguished by the uniform brown color of the dorsum (Fig. 5), instead presenting distinct dorsal contrasting markings (irregular brown blotches in *A. tapajos*, *A. crombiei*, and *A. magnussoni*). Furthermore, considering those species, *A. grillicantus* is distinguished by the yellowish colored ventral surface of head in live males (Fig. 5; grey-violaceous in *A. magnussoni*), by the presence of a pale whitish ventrolateral stripe (absent in *A. tapajos*), and by a body size smaller than *A. crombiei* (SVL 17.4–19.0 mm in males, 18.6–19.0 mm in females).

Another three cryptically colored *Allobates* share with *A. grillicantus* the uniform brown color of the dorsum, including its sister taxon *A. grillisimilis*. Of these, *A. grillicantus* is distinguished by the yellowish colored ventral surface of head in live males (Fig. 5; whitish-pinkish in *A. grillisimilis* and *A. caeruleodactylus*; grey-violaceous in *A. nunciatus*). Furthermore, considering these species, *A. grillicantus* is distinguished by the presence of a pale whitish ventrolateral stripe and cryptically colored dorsal surface of fingers (ventrolateral stripe absent and blue colored fingers in *A. caeruleodactylus*), and by a body size smaller than *A. nunciatus* (minimum SVL 19.2 mm) and larger than *A. grillisimilis* (SVL 12.8–15.9 in males, 12.8–16.0 in females).

The advertisement call of *A. grillicantus* is a trill consisting of series of short pulses (Table 2; Fig. 7; see call description section). Such a call structure distinguishes *A. grillicantus* from most of the compared species, whose calls form series of spaced units of repeated notes: *A. caeruleodactylus* and *A. magnussoni* (single notes); *A. tapajos* (mostly two notes) and *A. nunciatus* and *A. femoralis* (mostly four notes; Lima and Caldwell 2001; Lima et al. 2014, 2015; Simões et al. 2010). Among the compared *Allobates* emitting similar series of trills, *A. grillicantus* is distinguished by having a call of considerably shorter duration (0.15–0.51 s) and fewer elements per trill (3–15 pulses; 1.91–4.53 s, 25–59 notes in *A. crombiei* and 2.46–3.37 s, 10–14 notes in *A. tapajos*, which alternate between types of advertisement call and may emit trills; Lima et al. 2012, 2015).

The call structure of *A. grillicantus* is most similar to that of its sister taxon *A. grillisimilis*. In fact, most of the temporal parameters of the call of *A. grillicantus* overlap or differ only slightly from the known intraspecific variation of *A. grill-*

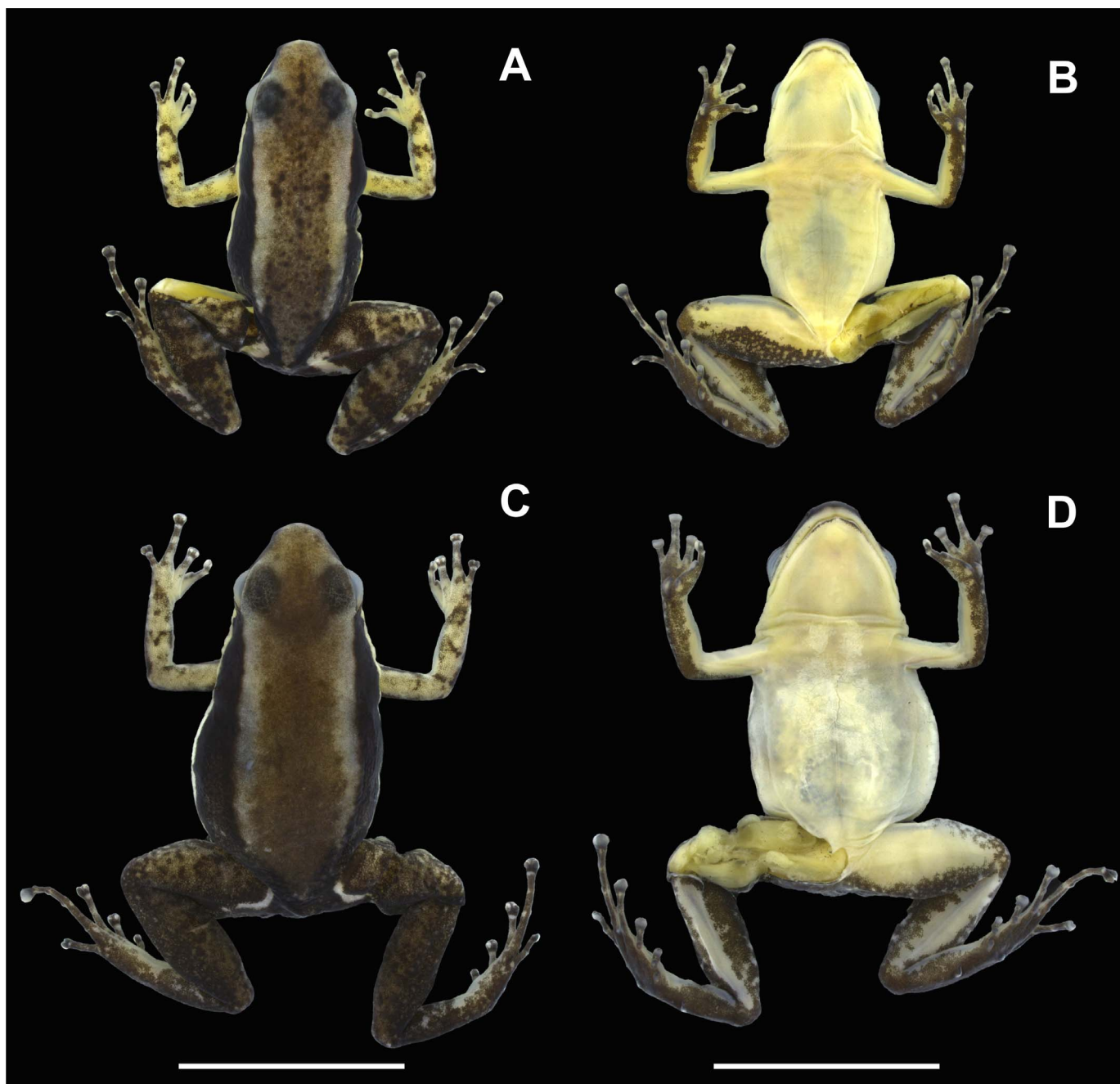


FIG. 2.—(A, B) Dorsal and ventral views of the preserved adult male holotype (MPEG 43046) and (C, D) female paratopotype (MPEG 43043) of *Allobates grillicantus*. Scale bar = 10.0 mm. Photographs by J. Magnusson. A color version of this figure is available online.

isimilis (from municipalities of Borba; type locality, Nova Olinda do Norte and Maués, state of Amazonas, Brazil; Simões et al. 2013b; Table 2). Acoustic divergence between *A. grillicantus* and *A. grillisimilis* is most evident in spectral parameters, such as the mean peak frequencies of the entire call, first pulse, central pulse, and last pulse, which promptly distinguishes *A. grillicantus* from topotypic *A. grillisimilis* (call 6394.2 ± 169.4 ; first pulse 6230.2 ± 185.3 ; central pulse 6434.9 ± 161.3 ; last pulse 6359.8 ± 146.3 ; Table 2; Fig. 8). However, the same parameters overlap with the known variation of *A. grillisimilis* from other localities. Comparing acoustic evidences from various localities of

occurrence of this species pair, an overall pattern of west-to-east decrease in the call frequency becomes apparent (Fig. 8). Despite this, a lower mean pulse emission rate clearly distinguishes the call of *A. grillicantus* from the full-range of known *A. grillisimilis* variation, which has faster calls (26.691–28.091 pulses/s; Table 2; Fig. 8).

Description of the holotype.—Adult male (Figs. 2–4), 16.4 mm SVL. Dorsum smooth laterally and with some scattered small granules centrally; granules distributed from the eye-level to the posterior region of dorsum, but more prominent at the level of arm insertion (in two opposite curved lines) and along the posterior region of dorsum;

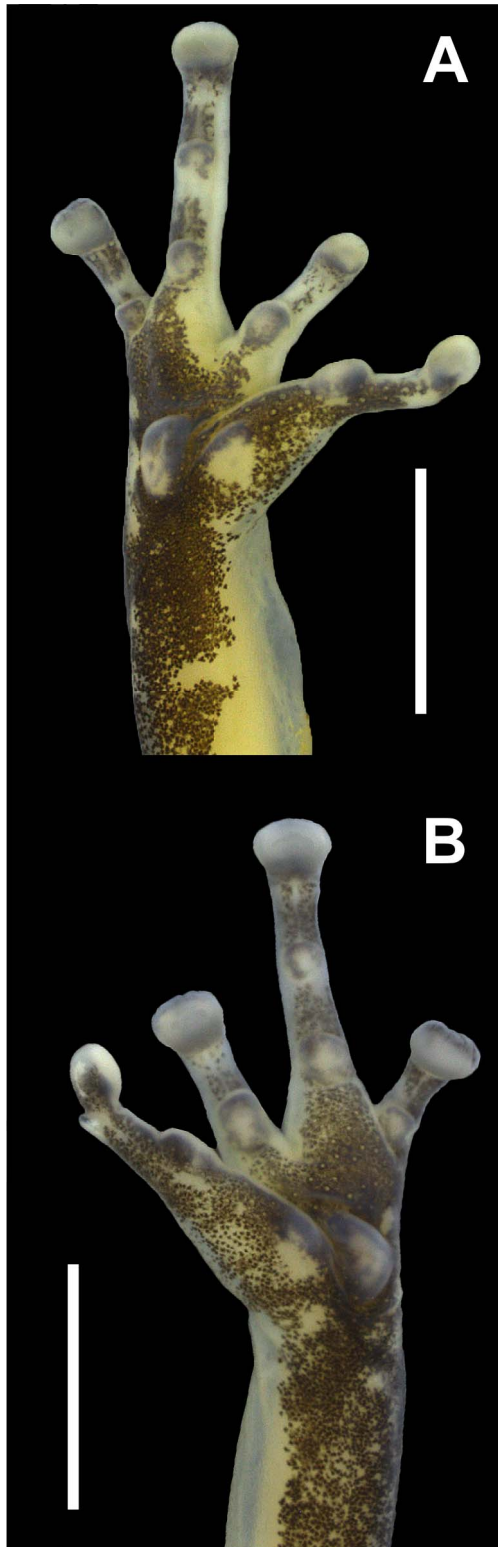


FIG. 3.—(A) Ventral surface of hand of the preserved adult male holotype (MPEG 43046) and (B) female paratopotype (MPEG 43043) of *Allobates grillicantus*. Scale bar = 2.0 mm. Photographs by J. Magnusson. A color version of this figure is available online.

throat and abdomen smooth (Fig. 2). Head approximately equal in width and length (HW = 98% of HL; HL = 34% of SVL); snout rounded in dorsal and lateral views, slightly shorter than eye diameter; *canthus rostralis* indistinct; loreal



FIG. 4.—(A) Ventral surface of feet of the preserved adult male holotype (MPEG 43046) and (B) female paratopotype (MPEG 43043) of *Allobates grillicantus*. Scale bar = 3.0 mm. Photographs by J. Magnusson. A color version of this figure is available online.

region obtuse; nares located posterolaterally to snout tip; eye diameter 46% of HL; tympanum distinct, with diameter shorter than half of the ED; tongue longer than wide, adhering anteriorly to floor of mouth; choanae relatively small, round; vomerine odontophores absent; a single subgular vocal sac.

Upper arm and forearm with approximately the same length; hand shorter than forearm; relative length of fingers IV < II < I < III; fingers with moderately expanded rounded tips; metacarpal tubercles present, inner metacarpal tubercle (thenar) weakly developed, oval to elliptic, outer metacarpal tubercle (palmar) large and drop-shaped; finger subarticular tubercles present and rounded, not exceeding the width of phalanges; one subarticular tubercle in fingers I, II, and IV and two in Finger III; supernumerary tubercles absent; Finger III with weakly developed preaxial swelling, with uniform width along the finger; width of the Finger III (at the level of third phalanx) shorter than the width of respective finger disc; lateral fringes absent on fingers (Fig. 3). Tibia longer than thigh, foot shorter than thigh and tibia; relative length of toes I < II < V < III < IV; basal webbing present between toes III and IV, webbing formula III $2^{1/2}$ – $3^{1/2}$ IV; toes with moderately expanded rounded tips; metatarsal tubercles present, inner elliptical and larger than the outer one, rounded; metatarsal fold absent; tarsal keel present, in form of a curved tubercle; toe subarticular tubercles present and rounded; one subarticular tubercle on toes I and II, two on toes III and V, and three on Toe IV, with the proximal tubercle on Toe IV considerably less developed (Fig. 4). Holotype measurements can be found in Table 1.

Coloration of the holotype in life.—Dorsum uniformly tan brown, with darker brown dots on the scattered granules. A continuous dark brown lateral stripe extends from the tip of snout to flanks and reaches the cloacal region. A pale whitish ventrolateral stripe delimits this dark stripe, extending from the arm insertion to groin. Pair of pale brown curved-shaped paracloacal marks present. Dorsal surfaces of arms tan brown, paler than color of dorsum; dorsal surfaces of legs greyish brown, with a contrasting aspect in relation to



FIG. 5.—Variation in color in life and external morphology of some adult specimens from the type series of *Allobates grillicantus* in dorsal, lateral, and ventral views (from left to right). (A) MPEG 43038, male, 15.7 mm snout-vent length (SVL); (B) INPA-H 41352, male, 15.8 mm SVL; (C) MPEG 43042, female, 17.7 mm SVL; (D) MPEG 43043, female, 17.7 mm SVL. Not to scale. Photographs by A.P. Lima.

dorsum color. Transversal distinct dark brown bars evident on forearms (two) and tibiae (three). Dorsal surfaces of hands and feet punctuated with occasional white dots. At ventral surface, chin and chest bright yellow; throat translucent pale yellow; abdomen pale yellow to slightly translucent, revealing a white peritoneum; forearms brown; upper arms pinkish to pale yellow; thighs and tibiae greyish white. Palmar surface of hands and plantar surface of feet uniformly brown. Iris metallic gold with fine black vermiculation; pupil black, with dark brown blotches in contact with its anterior and posterior part.

Coloration of holotype in preservative.—Dorsum dark brown centrally (Fig. 2) with darker brown dots on the scattered granules, and pale brown dorsolateral stripes. A continuous dark brown lateral stripe extends from the tip of

snout to flanks and reaches the cloacal region. A pale whitish-iridescent ventrolateral stripe delimits this dark stripe, extending from the arm insertion to groin. Pair of cream, curved paracloacal marks present. Dorsal surfaces of arms cream; dorsal surfaces of legs brown, at the same shade of the dorsum color. Transversal distinct dark brown bars evident in forearms (two) and weakly evident in tibiae (three). At ventral surfaces, chin, throat, chest, and abdomen cream; forearms, palms of hands, and soles of feet dark brown; upper arms and thighs translucent cream; tibiae greyish cream (Figs. 2–4).

External morphology variation.—The presence and development of Finger III preaxial swelling varies among adult males, but it is always weakly developed when present and uniformly distributed along the finger, and the width of

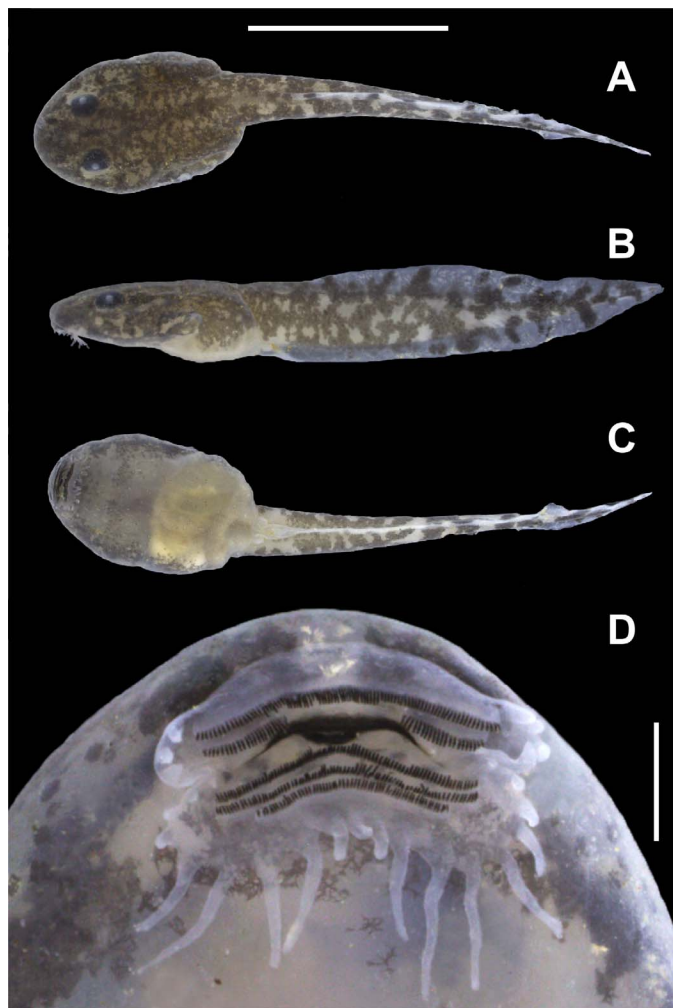


FIG. 6.—Dorsal (A), lateral (B), and ventral (C) views of a preserved tadpole of *Allobates grillicantus* and the detailed view of its oral disc (D). Tadpole in developmental stage 29 sensu Gosner (1960; from lot MPEG 43052). Scale bar = 5.0 mm (A–C); 0.5 mm (D). Photographs by J. Magnusson. A color version of this figure is available online.

the finger is always narrower than the width of the finger disc. As with the sister taxon *A. grillicantus*, *A. grillicantus* does not show evident sexual dimorphism in either the dorsal or ventral color pattern (Fig. 5). The brown color of the dorsum and arms varies between the shades of tan to reddish brown, and some individuals have darker spots on the tip of dorsal granules. Definition of the pale whitish ventrolateral stripe toward the ventral area varies among individuals, sometimes being diffuse or interrupted. On the dorsal surface of the arms and legs, there is a variable pattern of dark brown blotches, incomplete, or complete transverse bars. On the ventral surface of the body, yellow is always present but varies between shades of bright and pale yellow. Bright yellow areas may be restricted to the chin or be more widely distributed, reaching the middle of the abdomen. In some cases, the extension of pale yellow reaches the surfaces of the upper arms and the anterior region of the thighs. The throat is always translucent and consequently pale yellow,

contrasting with the surrounding shade of deeper yellow. The vocal sac of males is pale yellow when inflated (Fig. 10).

Tadpole description.—Measurements were obtained from 18 tadpoles at developmental stages 27 (from lot MPEG 43051), 29 (from lots MPEG 43052 and INPA-H 41357), and 31 (from lot MPEG 43053), and summarized in Table 3.

The following description is based on stage 29 larvae. Body ellipsoid in dorsal view, longer than wide, flattened in lateral view (Fig. 6). Body length 33% of TL; tail length 67% of TL; head width 85% of BW; body height 62% of BW; snout rounded in dorsal view and flattened in lateral view; eyes dorsal and directed laterally; eye–nostril distance 81% of ED; eye diameter 0.96 ± 0.06 mm; interorbital distance 51% of HW. Small naris located dorsolaterally and directed laterally; internarial distance 1.10 ± 0.07 mm. Sinistral spiracle as a free tube at midbody, with 0.55 ± 0.05 mm. Length of dextral vent tube 1.3 ± 0.20 mm. Dorsal fin begins posterior the body–tail insertion, with maximum height at approximately half of the caudal length. Ventral fin begins at body–tail insertion. Tail tip acuminate. Caudal musculature bifurcated dorsally, reaching anteriorly up to half of the body.

Oral disc positioned anteroventrally (Fig. 6), emarginated laterally, transversely elliptical, 1.71 ± 0.27 mm wide. Anterior labium with papillae absent anteriorly and three to four short and round papillae in a single row on each lateral margin. Posterior labium free from body wall, with a single row of marginal papillae. First four to five papillae adjacent from emargination small to moderately elongated, followed by eight very elongate, and three central moderately elongated. Upper jaw sheath flat medially, with lateral flexures, longer than the lower jaw sheath. Lower jaw sheath arc shaped, as deep as the upper jaw sheath. Cutting edge of upper and lower jaw sheaths serrated along the entire length. Labial tooth row formula 2(2) / 3(1); tooth Row A-1 complete, measuring 1.42 ± 0.19 mm in length; tooth Row A-2 interrupted medially, consisting of two widely separated rows at the level of upper jaw sheath, segments measuring 0.46 ± 0.07 mm in length and the gap measuring 0.50 ± 0.06 mm. Posterior tooth rows P-1 and P-2 with approximately the same length as Row A-1, with 1.30 ± 0.18 and 1.26 ± 0.19 mm, respectively, both longer than the complete P-3, with 0.92 ± 0.15 mm. This oral disc morphology (Fig. 6) was constant throughout all ontogenetic stages examined, but the number of marginal papillae on the posterior labium was slightly variable among individuals.

In preservative, color of dorsum, anterior part of the ventral area, and lateral surfaces with a pale cream background color, densely covered with dark brownish melanophores (Fig. 6), which aggregate in tail to form irregular brown blotches. Venter pale cream, with the posterior part translucent, and intestines visible through the skin. Tail fins translucent, with irregular brown blotches. The overall same coloration pattern occur in life (Fig. 10), but with the occurrence of iridescent golden dots at the dorsal, lateral, and anteroventral surfaces of the body. Shades of red and pink are also noticed in the body, as a result of internal organs and blood vessels being visible through translucent skin.

Comparison with tadpoles of other species.—The posterior labium surrounded by distinctly long marginal

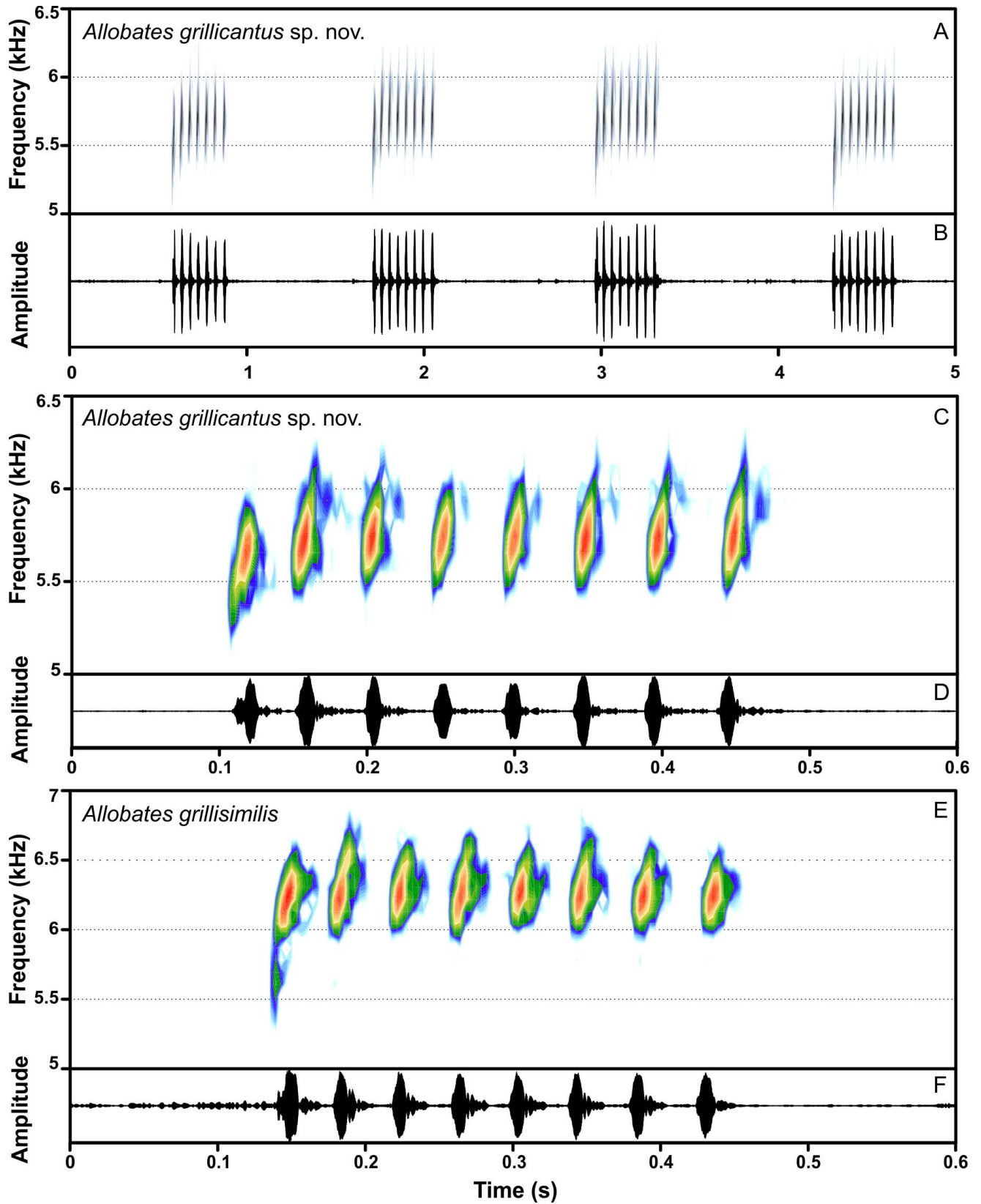


FIG. 7.—Spectrogram (above) and waveform (below) views of the advertisement call of *Allobates grillicantus* (A, B; holotype MPEG 43046, 16.4 mm snout-vent length), with a single eight-pulsed call zoomed at (C, D), compared with the same call arrangement from a topotypic specimen of its sister taxon *Allobates grillisimilis* (E, F). A color version of this figure is available online.

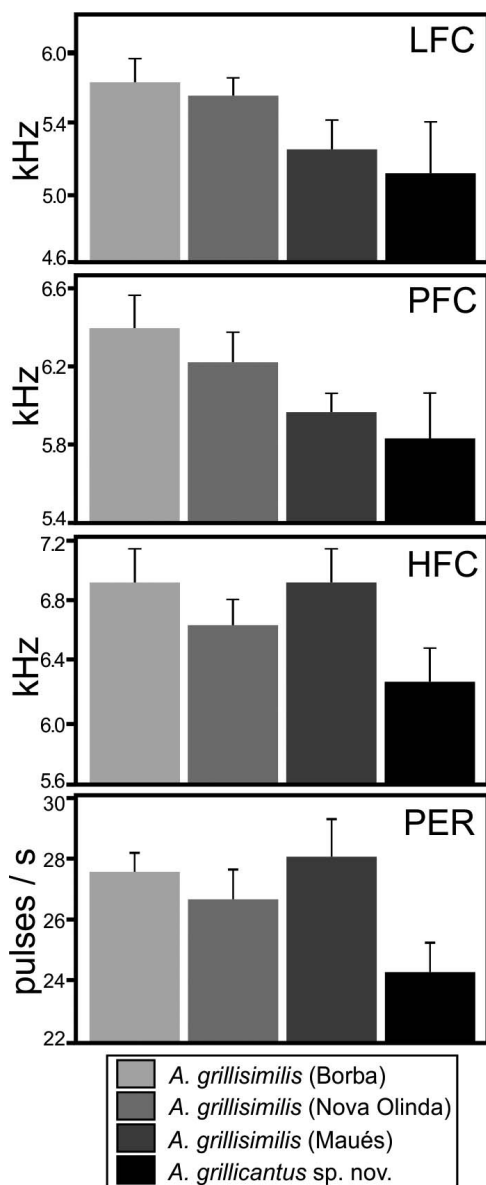


FIG. 8.—Spectral and temporal parameters useful for distinguishing the advertisement calls of *Allobates grillicantus* and its sister taxon *Allobates grillisimilis*, showing an overall decreasing west–east clinal pattern in call frequency (lowest [LFC], peak [PFC], and highest [HFC]), and highlighting the lower pulse emission rate (PER) in *A. grillicantus*. Values represent mean \pm standard deviation.

papillae distinguishes tadpoles of *A. grillicantus* from tadpoles of *A. femoralis*, *A. magnussoni*, and *A. nunciatus* (posterior labium with short papillae of similar size; Hero 1990; Lima et al. 2014; Moraes et al. 2019).

The posterior labium with long marginal papillae is shared with tadpoles of *A. caeruleodactylus*, *A. grillisimilis*, and *A. tapajos* (Caldwell et al. 2002; Simões et al. 2013b; Lima et al. 2015), but tadpoles of *A. grillicantus* are distinguished by the presence of a labial tooth Row P-3 shorter than P-1 and P-2 (P-3 with similar length to P-1 and P-2 in tadpoles of *A. grillisimilis*), by the length of P-3 surpassing half of the P-1 and P-2 length (P-3 extremely shorter, with total length not surpassing half of P-1 and P-2 length in tadpoles of *A. caeruleodactylus*), and by the presence of elongate papillae

distinctly longer than adjacent ones (moderately elongate in tadpoles of *A. tapajos*). Furthermore, compared with tadpoles of the sister taxon, *A. grillisimilis*, tadpoles of *A. grillicantus* have brown blotches that are more evident against the pale background, as a result of a greater density of melanophores (brown blotches less evident). Tadpoles have not been described for *A. crombiei*.

Advertisement call and variation.—The advertisement call of *A. grillicantus* resembles an insect stridulation (cricket-like) to the human ear and is formed by a series of trills followed by silent intervals of variable duration (Table 2; Fig. 7). The trills are composed of 3–15 short, closely spaced, pulses of very similar duration. Arrangements with 4 and 5 pulses were the most frequently emitted, corresponding to 258 of 643 (40%) analyzed calls in 11 distinct recordings. Three-pulsed calls can be considered as warm-up calls because they were emitted at beginning of series or when the individual was disturbed. Arrangements with 4–9 pulses correspond to 520 of 643 (81%) analyzed calls, but the species also emits arrangements with 10 (6%), 11 (2%), 12 (1.2%), 13 (0.6%), and 15 pulses (the rarest, 0.2%). Increases in pulse numbers per call seems positively correlated to excitement level in calling males, and such variation in pulse emission results in a mean call duration of 0.264 ± 0.073 s. Pulses have a slightly ascending frequency modulation, and slightly differ in spectral parameters across the emission, with the first pulse of each call generally emitted at a mean lower peak frequency (5817.3 ± 218.2 Hz), and showing mean higher frequency modulation (1025.2 ± 267.2 Hz) than central (peak frequencies 5843.5 ± 228.3 Hz and frequency modulation 890.3 ± 230.5 Hz) and last pulses (peak frequencies 5844.5 ± 230.6 Hz and frequency modulation 899.6 ± 246.0 Hz). Silent intervals between the calls are extremely variable, 0.865 ± 0.317 s long (range 0.411–1.677 s).

Geographic distribution.—*Allobates grillicantus* is only known from its type locality and a second nearby location, in the central-western Tapajós-Xingu interfluvium, close to municipalities of Trairão and Novo Progresso, state of Pará, Brazil (Fig. 9). However, we can predict that the distribution of the new species is greatly underestimated, especially due to the putative historical detection bias caused by its cryptic morphology and call. We estimate that *A. grillicantus* is likely to be more widely distributed throughout the Tapajós-Xingu interfluvium.

Natural history.—At the known localities of occurrence, *A. grillicantus* inhabits the leaf litter of primary and secondary nonflooded (*terra firme*) forests, with a high canopy and dense understory. The species was not recorded in naturally or anthropic-open habitats. The hot and humid climate of these ombrophilous forest localities provides an annual temperature ranging from 25°C to 28°C, with annual rainfall around 2000 mm (Alvares et al. 2013). Congeneric species syntopic to *A. grillicantus* include *A. femoralis*, *A. tapajos*, and *A. nunciatus*. *Allobates grillicantus* has a diurnal activity and was recorded breeding (Fig. 10) during the rainy season (March), with males calling mostly in the morning and late afternoon. Eggs are deposited in terrestrial nests, usually located on the inner surface of curled dead leaves on the leaf litter, but also recorded on upper surfaces of flat newly fallen green leaves (Fig. 10). The gelatinous egg-masses inside nests have a translucent aspect (Fig. 10), with

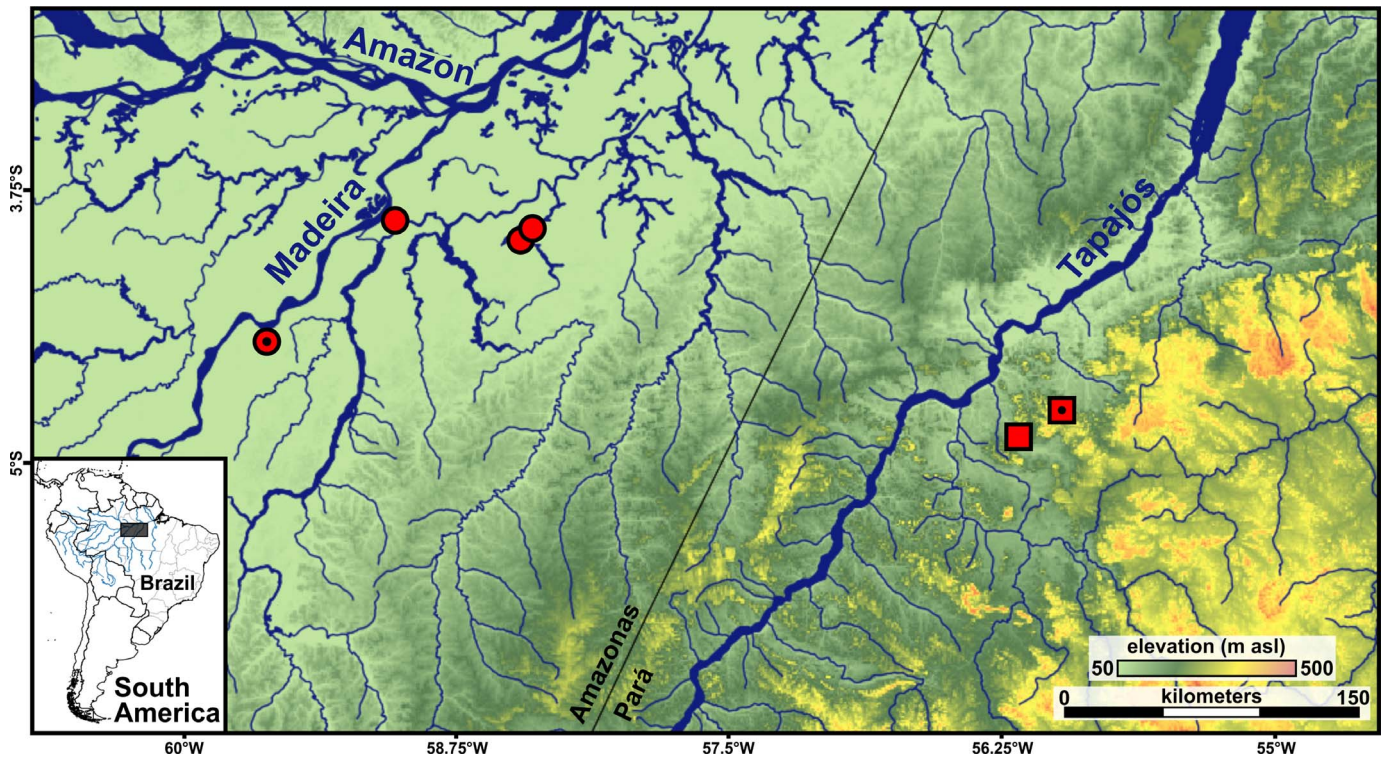


FIG. 9.—Geographic distribution of *Allobates grillicantus* (squares) and its sister taxon *Allobates grillisimilis* (dots) relative to the lower-middle courses of the Madeira River and the Tapajós River. Inset (lower left) shows the area within South America and Brazil. Dotted symbols indicate species' type localities. A color version of this figure is available online.

four egg-masses recorded containing 12, 12, 13, and 15 embryos. Two of these egg-masses were recorded at the same curled dead palm leaf. Only males were collected carrying developed tadpoles on the dorsum (INPA-H 41352,

MPEG 43045, 43048; 20 tadpoles on the dorsum of INPA-H 41352). Males deposit the tadpoles in nearby water bodies, such as puddles and standing water of nearby wetlands, where they complete the metamorphosis.



FIG. 10.—Reproductive behavior of *Allobates grillicantus* recorded at its type locality in the Middle Tapajós River region, state of Pará, Brazil. (A) Adult calling male (MPEG 43038); (B, C) gelatinous translucent egg-masses on curled dry fallen and newly fallen leaves in the forest leaf litter, with 15 and 12 embryos, respectively; (D, E) adult male recorded while transporting tadpoles (INPA-H 41352); (F) tadpole at developmental Stage 27 sensu Gosner (1960), showing color in life (from lot MPEG 43051). Photographs by A.P. Lima. A color version of this figure is available online.

DISCUSSION

Our description of *A. grillicantus* increases to 31 the number of nominal *Allobates* known to inhabit Brazilian Amazonia, although there is good evidence that this diversity is still greatly underestimating true values (Simões et al. 2018; Réjaud et al. 2020). With six nominal *Allobates* occurring on the riverbanks of the Middle Tapajós River (Frost 2019; present study), this region contains one of the highest alpha-diversities for this genus in Amazonia, even considering the entire Neotropical region (see Réjaud et al. 2020). The Middle Tapajós River region has extremely diverse regional biotas, with high levels of endemism for other groups of small frogs, such as the genus *Pristimantis*, *Adenomera* (Moraes et al. 2016; Carvalho et al. 2021), and *Amazophrynella* (Kaefer et al. 2019), as well as other vertebrates (Oliveira et al. 2016; Ribeiro-Júnior and Amaral 2016; Barrera-Guzmán et al. 2018). New inventories within the TRB, especially at its southern portion toward the upland region Serra do Cachimbo, are essential for discovering taxonomic novelties and understanding the overall patterns of *Allobates* distributions. Such increases in knowledge could also help illuminate the underlying processes generating and maintaining such a high diversity in the TRB.

Our molecular-based analysis of phylogenetic relationships mostly recovered the major clades within *Allobates*, discovered by recent large-scale phylogenetic inferences (Grant et al. 2017; Réjaud et al. 2020). Consequently, the new species, *A. grillicantus*, was also found to be nested within the following informal groups postulated by those studies: the cis-Andean 22-chromosome group (Grant et al. 2017), and the *A. caeruleodactylus* clade (Réjaud et al. 2020). The *A. caeruleodactylus* clade was nonmonophyletic in our analysis, and interrelationships among the major clades of *Allobates* also received lower support or slightly differed from those reported by these previous studies. However, such differences might be biased by the less comprehensive coverage of evolutionary sources and taxa sampling in our phylogeny (see Grant et al. 2017; Réjaud et al. 2020), and should be interpreted with caution. Despite such disagreements, our combined evidence of molecular and phenotypic similarities fully corroborate the position of *A. grillicantus*, from the east bank of the Tapajós River, as the sister taxon to *A. grillisimilis*, which occurs allopatrically on the west bank of this river (Simões et al. 2013b).

Since the description of *A. grillisimilis* (Simões et al. 2013b), a degree of genetic divergence has been noticed among its known populations, and this divergence is also reflected by subtle variations in body sizes and parameters of advertisement calls. However, further analyses of the external morphological variation of these populations did not expose sufficient divergence to justify any taxonomic changes (Simões et al. 2013b). Such a pattern indicates that the subdivisions in genetic and acoustic variation do not entail the existence of any distinct taxonomic entities, but instead suggest the occurrence of an incipient speciation process in *A. grillisimilis*, a process also noted for the congener *A. tapajos* (Maia et al. 2017). These diversification processes might be a result of the landscape dynamism of the interfluvium inhabited by *A. grillisimilis* (Madeira-Tapajós), which is known to generate intraspecific genetic structure for bird groups (Fernandes et al. 2014) and even other

Allobates, such as *A. masniger* (Tsuji-Nishikido et al. 2012; Moraes et al. 2019). Generation and maintenance of such intraspecific genetic clusters are generally associated (assuming allopatric divergences) with the emergence of geographic barriers, such as the largest rivers within the interfluvium (Fernandes et al. 2014). We predict that a similar pattern may have also occurred during the evolutionary history of the sister taxon *A. grillicantus*, and could well be clarified by the discovery of additional populations within the Tapajós-Xingu interfluvium.

When comparing the acoustic parameters emitted by distinct populations of *Allobates grillisimilis* and *A. grillicantus*, we noted a subtle west–east decrease in the mean peak frequency, resulting in a geographic cline pattern rather than abrupt changes. In contrast, when we compared the interfluvium of occurrence, the divergence in external morphology (given by ventral color) and molecular variation are abrupt: white vs. yellowish venter, and ca. 7–9% of genetic distance between the populations from Madeira-Tapajós and Tapajós-Xingu interfluviums. Discordances between phenotypic and molecular evolution are common events in the diversification of *Allobates* (e.g., Simões et al. 2010; Tsuji-Nishikido et al. 2012; Lima et al. 2014; Maia et al. 2017), and might be the result of distinct evolutionary rates and variable influences of combined modes of speciation, caused by the functional characteristics of *Allobates* species (e.g., small body size, low dispersal capacity, cryptic or aposematic mimic colors; Maia et al. 2017; Lima et al. 2020). This pattern of discordance illustrates the potential of the genus as a model for biogeographic studies that combine phenotypic and molecular data (Moraes et al. 2016; Réjaud et al. 2020).

The form and rates of calls are a relevant component for the intraspecific recognition of anurans (Amézquita et al. 2011), and the fact that the acoustic parameters of the *A. grillisimilis*–*A. grillicantus* species pair changes in a clinal pattern might indicate the occurrence of diversification processes at the population level. This observed pattern strongly suggests a role for genetic drift on allopatric divergence in this clade (Amézquita et al. 2009). We hypothesize that this is driven by the combined role of the establishment of a geographic barrier (Tapajós River) and an isolation by distance event, already established as relevant drivers of populational divergences in *Allobates* (Amézquita et al. 2009; Kaefer et al. 2013; Réjaud et al. 2020). Such diversification drivers might have eventually generated and maintained these two diagnosable evolutionary entities (morphologically and molecularly between riverbanks, and acoustically at the extremes of the known geographic distributions). Further studies that aim to understand the evolutionary history of the *A. grillisimilis*–*A. grillicantus* species pair, investigating dispersal routes, vicariant events, and current and past gene flow could formally test this hypothesis.

Regarding conservation status, the currently known geographic distribution of *A. grillicantus* is restricted to two localities in one of the areas most affected by deforestation in the Amazonia (Araújo et al. 2017). Such impacts are increasing exponentially, and are directly influenced by the recent anti-environmental policies and the fire crisis in this threatened biome (Pereira and Viola 2019). The increasing anthropic impact might negatively

affect the long-term viability of this new, forest-dependent, species, and further studies focused on its geographic distribution and population dynamics are needed for a better understanding of its conservation status.

Acknowledgments.—This study was funded by the Conselho Nacional de Desenvolvimento Científico e Tecnológico (A.P. Lima productivity fellowship and CNPq Universal, Grant #401120/2016-3). We thank to A.L.C. Prudente (MPEG), F.P. Werneck and A. Silva (INPA) for receiving the type series, and F.P. Werneck and A. Silva for granting access to specimens deposited at the Amphibians and Reptiles Collection (INPA-H). P.I. Simões and P.L.V. Peloso kindly provided original data used for the description of *A. grillisimilis*. W.E. Magnusson helped in the fieldwork and with filming species. J.L. Magnusson helped with specimen photographs and measurements. S.K. Woodley, J. Faivovich, P.R. Melo-Sampaio, M. Ferrão, and two anonymous reviewers provided valuable insights and suggestions throughout the development of the manuscript, T.R. Carvalho helped with the acoustic analyses, and A. Barnett helped with the English. The specimens were collected under collection Permit #13777 provided by the Instituto Chico Mendes de Conservação da Biodiversidade (ICMBio).

SUPPLEMENTAL MATERIAL

Supplemental material associated with this article can be found online at <https://doi.org/10.1655/Herpetologica-D-20-00010.S1> and <https://doi.org/10.1655/Herpetologica-D-20-00010.S2>

LITERATURE CITED

- Altig, R., and R.W. McDiarmid. 1999. Tadpoles, the Biology of Anuran Larvae. The University of Chicago Press, USA.
- Alvares, C.A., J.L. Stape, P.C. Sentelhas, J.L.M. Gonçalves, and G. Sparovek. 2013. Koppen's climate classification map for Brazil. *Meteorologische Zeitschrift* 22:711–728.
- Amézquita, A., A.P. Lima, R. Jehle, L. Castellanos, O. Ramos, A.J. Crawford, H. Gasser, and W. Hödl. 2009. Calls, colours, shapes, and genes: A multi-trait approach to the study of geographic variation in the Amazonian frog *Allobates femoralis*. *Biological Journal Linnean Society* 98:826–838.
- Amézquita, A., S.V. Flechas, A.P. Lima, H. Gasser, and W. Hödl. 2011. Acoustic interference and recognition space within a complex assemblage of dendrobatid frogs. *Proceedings of the National Academy of Sciences* 108:17058–17063.
- Araújo, E., P. Barreto, S. Baima, and M. Gomes. 2017. Unidades de Conservação mais Desmatadas da Amazônia Legal (2012–2015). Imazon, Brazil. [In Portuguese.] Available at <http://www.imazon.org.br/unidades-de-conservacao-mais-desmatadas-da-amazonia-legal-2012-2015/>. Accessed 12 April 2021.
- Barrera-Guzmán, A.O., A. Aleixo, M.D. Shawkey, and J.T. Weir. 2018. Hybrid speciation leads to novel male secondary sexual ornamentation of an Amazonian bird. *Proceedings of the National Academy of Sciences* 115:E218–E225.
- Boulenger, G.A. 1884. On a collection of frogs from Yurimaguas, Huallaga River, Northern Peru. *Proceedings of the Zoological Society of London* 1883:635–638.
- Boulenger, G.A. 1912. Descriptions of new batrachians from the Andes of South America, preserved in the British Museum. *Annals and Magazine of Natural History, Series 8*, 10:185–191.
- Caldwell, J.P., A.P. Lima, and G.M. Biavatia. 2002. Descriptions of tadpoles of *Colostethus marchesianus* and *Colostethus caeruleodactylus* (Anura: Dendrobatidae) from their type localities. *Copeia* 1:166–172.
- Caminer, M.A., and S.R. Ron. 2014. Systematics of treefrogs of the *Hypsiboas calcaratus* and *Hypsiboas fasciatus* species complex (Anura, Hylidae) with the description of four new species. *ZooKeys* 370:1–68.
- Carvalho T.R., L.J.C.L. Moraes, A.P. Lima, . . . C.F.B. Haddad. 2021. Systematics and historical biogeography of Neotropical foam-nesting frogs of the *Adenomera heyeri* clade (Leptodactylidae), with the description of six new Amazonian species. *Zoological Journal of the Linnean Society* 191:395–433.
- Ferrão, M., O. Colatreli, R. Fraga, I.L. Kaefer, J. Moravec, and A.P. Lima. 2016. High species richness of *Scinax* treefrogs (Hylidae) in a threatened Amazonian landscape revealed by an integrative approach. *PLOS ONE* 11:e0165679. DOI: <https://dx.doi.org/10.1371/journal.pone.0165679>.
- Ferrão, M., J. Moravec, L.J.C.L. Moraes, V.T. de Carvalho, and M. Gordo. 2019. Rediscovery of *Osteocephalus vilarsi* (Anura: Hylidae): An overlooked but widespread Amazonian spiny-backed treefrog. *PeerJ* 7:e8160. DOI: <https://dx.doi.org/10.7717/peerj.8160>.
- Fernandes, A.M., M. Cohn-Haft, T. Hrbek, and I.P. Farias. 2014. Rivers acting as barriers for bird dispersal in the Amazon. *Revista Brasileira de Ornitologia* 22:363–373.
- Frost, D.R. 2019. Amphibian Species of the World: An Online Reference, Version 6.0. American Museum of Natural History, USA. Available at <https://amphibiansoftheworld.amnh.org>. Accessed 12 Apr 2021.
- Gosner, K.L. 1960. A simplified table for staging anuran embryos and larvae with notes on identification. *Herpetologica* 16:183–190.
- Grant, T., D.R. Frost, J.P. Caldwell, R. Gagliardo, C.F.B. Haddad, P.J.R. Kok, D.B. Means, B.P. Noonan, W.E. Schargel, and W.C. Wheeler. 2006. Phylogenetic systematics of dart-poison frogs and their relatives (Anura: Athesphatanura: Dendrobatidae). *Bulletin of the American Museum of Natural History* 299:1–262.
- Grant, T., M. Rada, M.A. Anganoy-Criollo, A. Batista, P.H.S. Dias, A.M. Jeckel, D.J. Machado, and J.V. Rueda-Almonacid. 2017. Phylogenetic systematics of dart-poison frogs and their relatives revisited (Anura: Dendrobatoidea). *South American Journal of Herpetology* 12:1–90. DOI: <https://dx.doi.org/10.2994/SAJH-D-17-00017.1>.
- Hero, J.-M. 1990. An illustrated key to tadpoles occurring in the Central Amazon rainforest, Manaus, Amazonas, Brasil. *Amazoniana* 11:201–262.
- Jaramillo, A.F., I. de La Riva, J.M. Guayasami, J.C. Chaparro, G. Gagliardi-Urrutia, R.C. Gutiérrez, I. Brcko, C. Vilà, and S. Castroviejo-Fisher. 2020. Vastly underestimated species richness of Amazonian salamanders (Plethodontidae: *Bolitoglossa*) and implications about plethodontid diversification. *Molecular Phylogenetics and Evolution* 149:106841.
- Kaefer, I.L., B.M. Tsuji-Nishikido, E.P. Mota, I.P. Faria, and A.P. Lima. 2013. The early stages of speciation in Amazonian forest frogs: Phenotypic conservatism despite strong genetic structure. *Evolutionary Biology* 40:228–245.
- Kaefer, I.L., R.R. Rojas-Zamora, M. Ferrão, I.P. Farias, and A.P. Lima. 2019. A new species of *Amazophrynella* (Anura: Bufonidae) with two distinct advertisement calls. *Zootaxa* 4577:316–334.
- Katoh, K., and D.M. Standley. 2013. MAFFT Multiple sequence alignment software version 7: Improvements in performance and usability. *Molecular Biology and Evolution* 30:772–780.
- Kearse, M., R. Moir, A. Wilson, . . . A. Drummond. 2012. Geneious Basic: An integrated and extendable desktop software platform for the organization and analysis of sequence data. *Bioinformatics* 28:1647–1649.
- Köhler, J., M. Jansen, A. Rodríguez, P.J.R. Kok, L.F. Toledo, M. Emmrich, F. Glaw, C.F.B. Haddad, M.O. Rödel, and M. Vences. 2017. The use of bioacoustics in anuran taxonomy: Theory, terminology, methods and recommendations for best practice. *Zootaxa* 4251:1–124.
- Kumar, S., G. Stecher, and K. Tamura. 2016. MEGA7: Molecular evolutionary genetics analysis version 7.0 for bigger datasets. *Molecular Biology and Evolution* 33:1870–1874.
- La Marca, E., J. Manzanilla, and A. Mijares-Urrutia. 2004. Revisión taxonómica del *Colostethus* del Norte de Venezuela confundido durante largo tiempo con *C. brunneus*. *Herpetotropicos* 1:40–50. [In Spanish.]
- Lanfear, R., P.B. Frandsen, A.M. Wright, T. Senfeld, and B. Calcott. 2017. PartitionFinder 2: New methods for selecting partitioned models of evolution for molecular and morphological phylogenetic analyses. *Molecular Biology and Evolution* 34:772–773.
- Ligges, U., S. Krey, O. Mersmann, and S. Schnackenberg. 2018. tuneR: Analysis of Music and Speech, Version 1.3.3. R Foundation for Statistical Computing, Austria. Available at <https://CRAN.R-project.org/package=tuneR>. Accessed 12 April 2021.
- Lima, A.P., and J.P. Caldwell. 2001. A new Amazonian species of *Colostethus* with sky blue digits. *Herpetologica* 57:133–138.
- Lima, A.P., D.E.A. Sanchez, and J.R.D. Souza. 2007. A new Amazonian species of the frog genus *Colostethus* (Dendrobatidae) that lays its eggs on the undersides of leaves. *Copeia* 2007:114–122.
- Lima, A.P., L.K. Erdtmann, and A. Amézquita. 2012. Advertisement call and colour in life of *Allobates crombiei* (Morales) “2000” [2002] (Anura: Aromobatidae) from the type Locality (Cachoeira do Espelho), Xingu River, Brazil. *Zootaxa* 3475:86–88.
- Lima, A.P., P.I. Simões, and I.L. Kaefer. 2014. A new species of *Allobates* (Anura: Aromobatidae) from the Tapajós River basin, state of Pará, Brazil. *Zootaxa* 3889:355–387.
- Lima, A.P., P.I. Simões, and I.L. Kaefer. 2015. A new species of *Allobates* (Anura: Aromobatidae) from Parque Nacional da Amazônia, state of Pará, Brazil. *Zootaxa* 3980:501–525.
- Lima, A.P., M. Ferrão, and D.L. Silva. 2020. Not as widespread as thought:

- Integrative taxonomy reveals cryptic diversity in the Amazonian nurse frog *Allobates tinae* Melo-Sampaio, Oliveira & Prates, 2018 and description of a new species. *Journal of Zoological Systematics and Evolutionary Research* 58:1173–1194.
- Lutz, A. 1925. Batracienses do Brasil. *Comptes Rendus et Mémoires Hebdomadaires des Séances de la Société de Biologie et des ses Filiales*, Paris 93:137–139. [In French.]
- Lyra, M.L., C.F.B. Haddad, and A.M.L. Azeredo-Espin. 2017. Meeting the challenge of DNA barcoding Neotropical amphibians: Polymerase chain reaction optimization and new COI primers. *Molecular Ecology Resources* 17:966–980.
- Maia, G.F., A.P. Lima, and I.L. Kaefer. 2017. Not just the river: Genes, shapes, and sounds reveal population-structured diversification in the Amazonian frog *Allobates tapajós* (Dendrobatoidea). *Biological Journal of the Linnean Society* 121:95–108.
- Martins, M. 1989. Nova espécie de *Colostethus* da Amazônia central (Amphibia: Dendrobatidae). *Revista Brasileira de Biologia* 49:1009–1012. [In Spanish.]
- Melo-Sampaio, P.R., R.M. Oliveira, and I. Prates. 2018. A new nurse frog from Brazil (Aromobatidae: *Allobates*), with data on the distribution and phenotypic variation of western Amazonian species. *South American Journal of Herpetology* 13:131–149. DOI: <https://dx.doi.org/10.2994/SAJH-D-17-00098.1>.
- Melo-Sampaio, P.R., I. Prates, P.L.V. Peloso, R. Recoder, F. Dal Vechio, S. Marques-Souza, and M.T. Rodrigues. 2020. A new nurse frog from Southwestern Amazonian highlands, with notes on the phylogenetic affinities of *Allobates alessandroi* (Aromobatidae). *Journal of Natural History* 53:1–20.
- Moraes, L.J.C.L., D. Pavan, M.C., Barros and C.C. Ribas. 2016. The combined influence of riverine barriers and flooding gradients on biogeographical patterns for amphibians and squamates in south-eastern Amazonia. *Journal of Biogeography* 43:2113–2124.
- Moraes, L.J.C.L., A.P. Almeida, R. Fraga, R.R. Rojas-Zamora, R.M. Pirani, A.A.A. Silva, V.T. Carvalho, M. Gordo, and F.P. Werneck. 2017. Integrative overview of the herpetofauna from Serra da Mocidade, a granitic mountain range in northern Brazil. *ZooKeys* 715:103–159.
- Moraes, L.J.C.L., D. Pavan, and A.P. Lima. 2019. A new nurse frog of *Allobates masniger-nidicola* complex (Anura, Aromobatidae) from the east bank of Tapajós River, eastern Amazonia. *Zootaxa* 4648:401–434.
- Moraes, L.J.C.L., C.C. Ribas, D. Pavan, and F.P. Werneck. 2020. Biotic and landscape evolution in an Amazonian contact zone: Insights from the herpetofauna of the Tapajós River basin. Pp. 683–712 in *Neotropical Diversification: Patterns and Processes* (V. Rull and A. Carnaval, eds.). Springer, USA.
- Morales, V.R. 1994. Taxonomía sobre algunos *Colostethus* (Anura: Dendrobatidae) de Sudamérica, con descripción de dos especies nuevas. *Revista Española de Herpetología* 8:95–103. [In Spanish.]
- Morales, V.R. 2002 [2000]. Sistemática y biogeografía del grupo *trilineatus* (Amphibia, Anura, Dendrobatidae, *Colostethus*), con descripción de once nuevas especies. *Publicaciones de la Asociación de Amigos de Doñana* 13:1–59. [In Spanish.]
- Myers, C.W., and M. A. Donnelly. 2001. Herpetofauna of the Yutajé–Corocoro Massif, Venezuela: Second report from the Robert G. Goelt American Museum–TerraMar Expedition to the northwestern tepuis. *Bulletin of the American Museum of Natural History* 261:1–85.
- Myers, C.W., A. Paolillo-O. and J.W. Daly. 1991. Discovery of a defensively malodorous and nocturnal frog in the family Dendrobatidae: Phylogenetic significance of a new genus and species from Venezuelan Andes. *American Museum Novitates* 3002:1–33.
- Oliveira, T.G., D. Mazim, O.Q. Vieira, ... C. Lima-Miranda. 2016. Nonvolant mammal megadiversity and conservation issues in a threatened Central Amazonian hotspot in Brazil. *Tropical Conservation Science* 9:1–16. DOI: <https://dx.doi.org/10.1177/1940082916672340>.
- Padial, J.M., A.D. Miralles, I. De la Riva, and M. Vences. 2010. The integrative future of taxonomy. *Frontiers in Zoology* 7:1–14. DOI: <https://dx.doi.org/10.1186/1742-9994-7-16>.
- Palumbi, S.R., A.P. Martin, S. Romano, W.O. McMillan, L. Stice, and G. Grabowski. 1991. *The Simple Fool's Guide to PCR*. University of Hawaii Press, USA.
- Pereira, J.C., and E. Viola. 2019. Catastrophic climate risk and Brazilian Amazonian politics and policies: A new research agenda. *Global Environmental Politics* 19:93–103.
- R Core Team. 2019. R: A Language and Environment for Statistical Computing, Version 3.6.1. R Foundation for Statistical Computing, Austria. Available at <http://www.r-project.org/>. Accessed 12 April 2021.
- Rambaut, A., A.J. Drummond, D. Xie, G. Baele, and M.A. Suchard. 2018. Posterior summarisation in Bayesian phylogenetics using Tracer 1.7. *Systematic Biology* 67:901–904.
- Réjaud, A., M.T. Rodrigues, A.J. Crawford, ... A. Fouquet. 2020. Historical biogeography identifies a possible role of the Pebas system in the diversification of the Amazonian rocket frogs (Aromobatidae: *Allobates*). *Journal of Biogeography* 47:2472–2482.
- Ribeiro-Júnior, M.A., and S. Amaral. 2016. Diversity, distribution, and conservation of lizards (Reptilia: Squamata) in the Brazilian Amazonia. *Neotropical Biodiversity* 2:195–421. DOI: <https://dx.doi.org/10.1080/23766808.2016.1236769>.
- Rivero, J.A. 1980 [1978]. Notas sobre los anfibios de Venezuela III. Nuevos *Colostethus* de los Andes Venezolanos. *Memoria. Sociedad de Ciencias Naturales La Salle* 38:95–111. [In Spanish.]
- Ronquist, F., M. Teslenko, P. van der Mark, D.L. Ayres, A. Darling, S. Höhna, B. Larget, L. Liu, M.A. Suchard, and J.P. Huelsenbeck. 2012. MrBayes 3.2: Efficient Bayesian phylogenetic inference and model choice across a large model space. *Systematic Biology* 61:539–542.
- Santos, J.C., M. Baquero, C. Barrio-Amorós, L.A. Coloma, L.K. Erdtmann, A.P. Lima, and D.C. Cannatella. 2014. Aposematism increases acoustic diversification and speciation in poison frogs. *Proceedings of the Royal Society B: Biological Sciences* 281:20141761.
- Savage, J.M., and W.R. Heyer. 1997. Digital webbing formulae for anurans: A refinement. *Herpetological Review* 28:131.
- Simões, P.I. 2016. A new species of nurse-frog (Aromobatidae, *Allobates*) from the Madeira River basin with a small geographic range. *Zootaxa* 4083:501–525.
- Simões, P.I., A.P. Lima, and I.P. Farias. 2010. The description of a cryptic species related to the pan-Amazonian frog *Allobates femoralis* (Boulenger 1883) (Anura: Aromobatidae). *Zootaxa* 2406:1–28.
- Simões, P.I., I.L. Kaefer, I.P. Farias, and A.P. Lima. 2013a. An integrative appraisal of the diagnosis and distribution of *Allobates sumtuosus* (Morales, 2002) (Anura, Aromobatidae). *Zootaxa* 3746:401–421.
- Simões, P.I., M.J. Sturaro, P.L.V. Peloso, and A.P. Lima. 2013b. A new diminutive species of *Allobates* Zimmermann and Zimmermann, 1988 (Anura, Aromobatidae) from the northwestern Rio Madeira–Rio Tapajós interfluvium, Amazonas, Brazil. *Zootaxa* 3609:251–273.
- Simões, P.I., L.A.G. Gagliardi-Urrutia, F.J.M. Rojas-Runjaic, and S. Castroviejo-Fisher. 2018. A new species of nurse-frog (Aromobatidae, *Allobates*) from the Juami River basin, northwestern Brazilian Amazonia. *Zootaxa* 4387:109–133.
- Simões, P.I., D. Rojas, and A.P. Lima. 2019. A name for the nurse-frog (*Allobates*, Aromobatidae) of Floresta Nacional de Carajás, Eastern Brazilian Amazonia. *Zootaxa* 4550:71–100.
- Souza, J.R.D., M. Ferrão, J. Hanken, and A. P. Lima. 2020. A new nurse frog (Anura: *Allobates*) from Brazilian Amazonia with a remarkably fast multi-noted advertisement call. *PeerJ* 8:e9979. DOI: <https://dx.doi.org/10.7717/peerj.9979>.
- Sueur, J., T. Aubin, and C. Simonis. 2008. seewave: A free modular tool for sound analysis and synthesis. *Bioacoustics* 18:213–226.
- Tsuji-Nishikido, B.M., I.L. Kaefer, F.C. Freitas, M. Menin, and A.P. Lima. 2012. Significant but not diagnostic: Differentiation through morphology and calls in the Amazonian frogs *Allobates nidicola* and *A. masniger*. *Herpetological Journal* 22:105–114.
- Vacher, J.P., P.J.R. Kok, M.T. Rodrigues, ... A. Fouquet. 2017. Cryptic diversity in Amazonian frogs: Integrative taxonomy of the genus *Anomaloglossus* (Amphibia: Anura: Aromobatidae) reveals a unique case of diversification within the Guiana Shield. *Molecular Phylogenetics and Evolution* 112:158–173.
- Vences, M., Z.T. Nagy, G. Sonet, and E. Verheyen. 2012. DNA barcoding amphibians and reptiles. Pp. 79–107 in *DNA Barcodes: Methods and Protocols, Methods in Molecular Biology*, Volume 858 (W.J. Kress and D.L. Erickson, eds.). Humana Press, USA.
- Werner, F. 1899. Ueber Reptilien und Batrachier aus Columbien und Trinidad. *Verhandlungen des Zoologisch-Botanischen Vereins in Wien* 49:470–484. [In German.]

Accepted on 1 February 2021

ZooBank.org registration LSID: [urn:lsid:zoobank.org:pub:D8417153-E9C8-4CAS-BC70-3FF3735CE76A](https://zoobank.org/pub:D8417153-E9C8-4CAS-BC70-3FF3735CE76A)

Published on 8 June 2021

Associate Editor: Julian Faivovich

APPENDIX

Specimens Examined

Allobates bacurau.—Adults ($n = 13$). BRAZIL: AMAZONAS: Estrada do Miriti, Manicoré: INPA-H 35398 (holotype), 35397, 35399–35409 (paratypes).

Allobates brunneus.—Adults ($n = 38$). BRAZIL: MATO GROSSO: NE of Chapada dos Guimarães: INPA-H 10111–48 (topotypes). Tadpoles ($n = 15$). BRAZIL: MATO GROSSO: NE of Chapada dos Guimarães: INPA-H 10025–10027, 10029–10030, 10032–10037, 10039, 10041, 10043, 10044 (topotypes).

Allobates caeruleodactylus.—Adults ($n = 17$). BRAZIL: AMAZONAS: Km 12 on the road to Autazes: INPA-H 7238 (holotype), 7229–7232, 7234–7237 (paratypes). Tadpoles ($n = 11$). BRAZIL: AMAZONAS: Km 12 on the road to Autazes: INPA-H 8037–8046, INPA-H 8085.

Allobates caldwella.—Adults ($n = 25$). BRAZIL: AMAZONAS: Careiro: RAPELD M1 at km 32 of the Brazilian federal highway BR-319: INPA-H 41047 (holotype), 41045–41046, 41049–41053, 41055–41057, 41059, 41061, 41063, 41067–41069 (paratopotypes); Km 12 of the Brazilian federal highway BR-319: INPA-H 41054, 41058, 41064, 41066 (paratypes); RAPELD M2, at km 100 of the Brazilian federal highway BR-319: INPA-H 41048, 41060, 41062, 41065 (paratypes).

Allobates carajas.—Adults ($n = 19$). BRAZIL: PARÁ: Floresta Nacional de Carajás: INPA-H 38643 (holotype), 38633, 38635, 38637, 38640–38642, 38646, 38647, 38649 (paratopotypes), 38624, 38634, 38636, 38638, 38639, 38644, 38645, 38648, 38650 (paratypes). Tadpoles ($n = 13$). BRAZIL: PARÁ: Floresta Nacional de Carajás: Lot INPA-H 38632.

Allobates crombiei.—Adults ($n = 11$). BRAZIL: PARÁ: Cachoeira do Espelho: INPA-H 30457–30477 (topotypes).

Allobates femoralis.—Adults ($n = 39$). BRAZIL: PARÁ: Treviso: INPA-H 11657–11671, 15232, 30769–30778; Itaituba: INPA-H 26342–26354.

Allobates fuscillus.—Adults ($n = 6$). BRAZIL: AMAZONAS: Ipixuna: Penedo, east bank of Juruá River: INPA-H 2532 (holotype), 2531 (paratopotype). Itamarati: Jaiú, Juruá River: INPA-H 3114, 3250, 3270, 3514 (paratypes).

Allobates gasconi.—Adults ($n = 18$). BRAZIL: AMAZONAS: Itamarati: Jaiú, west bank of Juruá River: INPA-H 3082 (holotype), 3073, 3079, 3085, 3090, 3150, 3151, 3172, 3249, 3406, 3415, 3483, 3484, 3491, 3494, 3496, 3512, 3513 (paratypes).

Allobates grillisimilis.—Adults ($n = 45$). BRAZIL: AMAZONAS: Borba: INPA-H 30779 (holotype), 30780–30808 (paratopotypes); Nova Olinda do Norte: INPA-H 30809–30823 (paratypes). Tadpoles ($n = 91$). BRAZIL: AMAZONAS: Borba: Lots INPA-H 30824–30828.

Allobates hodli.—Adults ($n = 102$). BRAZIL: ACRE: Fazenda Experimental Catuaba: INPA-H 11621–11640 (paratypes); Rondônia: Cachoeira do Jirau: INPA-H 16555 (holotype), 16541–16554, 16556–16569 (paratopotypes); Near Fortaleza do Abunã: INPA-H 16578, 16584–16587, 16589, 16591, 16592, 16597, 16602, 16603, 16605–16607, 16611–16614, 16620–16624, 16626, 16628, 16631, 16633, 16636, 16637, 16639–16641, 16643, 16645, 16646, 16648; Near Mutum-Paraná: INPA-H 16596, 16730, 16739, 16756, 16758, 16767, 16771, 16777, 16778, 16788, 16805, 16818, 16819 (paratypes).

Allobates magnussoni.—Adults ($n = 36$). BRAZIL: PARÁ: Parque Nacional da Amazônia: INPA-H 32960 (holotype), 32961–32976, 32978–32982 (paratopotypes); Treviso: INPA-H 10105–10109, 33930–33934; Jamanxim: INPA-H 33935 (paratypes). Tadpoles ($n = 7$). BRAZIL: PARÁ: Treviso: INPA-H 10054, 10056, 10058, 10059, 10060; Parque Nacional da Amazônia: INPA-H 32983, 33936.

Allobates marchesianus.—Adults ($n = 41$). BRAZIL: AMAZONAS: Missão

Taracua: INPA-H 7959–7990 (topotypes); São Gabriel da Cachoeira, 175 km E Missão Taracua: INPA-H 7991, 7993, 8000–8007). Tadpoles ($n = 11$). BRAZIL: AMAZONAS: Missão Taracua: INPA-H 7943–7950, 7992, 7998, 8084 (topotypes).

Allobates masniger.—Adults ($n = 96$). BRAZIL: AMAZONAS: Borba: INPA-H 28075–28078, 28084, 28089, 28092, 28095, 28098, 28100, 28104, 28105, 28112, 28114, 28119; Novo Aripuanã: INPA-H 28054–28056, 28058–28060, 28062–28067, 28069, 28072–28074, 28080, 28083, 28086–28091, 28096, 28097, 28101, 28108, 28117; Road to Apuí: INPA-H 28057, 28061, 28068, 28071, 28076, 28079, 28081, 28085, 28102, 28106, 28109, 28116, 28190, 28191; PARÁ: Parque Nacional da Amazônia: INPA-H 28195–28217 (topotypes); Jacareacanga: INPA-H 28053, 28070, 28077, 28082, 28093, 28094, 28099, 28103, 28107, 28110, 28111, 28113, 28115, 28118, 28120.

Allobates myersi.—Adults ($n = 8$). BRAZIL: AMAZONAS: São Gabriel da Cachoeira: INPA-H 26369–26372, 26374, 26376, 26377, 26379.

Allobates nidicola.—Adults ($n = 80$). BRAZIL: AMAZONAS: Km 12 on road to Autazes: INPA-H 8093 (holotype), 7253–7259, 7261, 7262, 8094 (paratypes), INPA-H 28122, 28124, 28127, 28129, 28131, 28144, 28159, 28163, 28166, 28169, 28171, 28172, 28174, 28179, 28184, 28185 (topotypes); BR-319, Km 260: INPA-H 28126, 28133, 28153, 28156, 28168, 28173, 28175, 28178, 28181, 28183, 28186, 28189; PPBio Manaquiri: INPA-H 28137, 28140, 28143, 28146, 28148, 28155, 28157, 28160, 28162, 28164, 28167, 28170, 28176, 28182, 28187; BR-319 Tupana: INPA-H 28128, 28130, 28134, 28136, 28141–28142, 28145, 28151–28152, 28161, 28174, 28177, 28188; Vila Gomes: 28121, 28123, 28125, 28132, 28135, 28138–28139, 28147, 28149, 28150, 28154, 28158, 28165, 28180. Tadpoles ($n = 16$). BRAZIL: AMAZONAS: Km 12 on road to Autazes: INPA-H 8021–8033, 8137–8139.

Allobates nunciatus.—Adults ($n = 20$). BRAZIL: PARÁ: East bank of Middle Tapajós River: INPA-H 40486 (holotype), 40305, 40307, 40308, 40320, 40324, 40474–40485, 40488, 40489 (paratypes). Tadpoles ($n = 12$). BRAZIL: PARÁ: East bank of Middle Tapajós River: Lot INPA-H 40487.

Allobates paleovarzensis.—Adults ($n = 45$). BRAZIL: AMAZONAS: Careiro da Várzea: INPA-H 20904 (holotype), 20861–20903, 20905 (paratypes).

Allobates subfolionidificans.—Adults ($n = 30$). BRAZIL: ACRE: Parque Zoológico de Universidade Federal do Acre: INPA-H 13760 (holotype), 11958–11974, 13749–13754, 13756–13759, 13761, 13762 (paratypes). Tadpoles ($n = 2$). BRAZIL: ACRE: Parque Zoológico de Universidade Federal do Acre: INPA-H 14822, 14823.

Allobates sumtuosus.—Adults ($n = 11$). BRAZIL: AMAZONAS: Reserva Florestal Adolpho Ducke: INPA-H 31949–31951; PARÁ: Reserva Biológica do Rio Trombetas: INPA-H 31952–56, INPA-H 31958–60 (topotypes).

Allobates tapajos.—Adults ($n = 24$). BRAZIL: PARÁ: Parque Nacional da Amazônia: INPA-H 34425 (holotype), 34402–34424 (paratypes). Tadpoles ($n = 2$). BRAZIL: PARÁ: Parque Nacional da Amazônia: Lots INPA-H 34426, 34427.

Allobates tinae.—Adults ($n = 27$). BRAZIL: ACRE: Boca do Acre: INPA-H 40976, 41022, 41027, 41037, 41040; Rondônia: Porto Velho, west bank of upper Madeira River: INPA-H 41012–21, 41029–36, 41041–44.

Allobates trilineatus.—Adults ($n = 36$). BRAZIL: ACRE: Parque Zoológico de Universidade Federal do Acre: INPA-H 11958–11993.

Allobates velocicantus.—Adults ($n = 13$). BRAZIL: ACRE: Mâncio Lima: INPA-H 41342 (holotype), INPAH 41338–41341, 41343–41349 (paratopotypes); Cruzeiro do Sul: road connecting Cruzeiro do Sul to Guajará: INPA-H 41350 (paratype).

Allobates vanzolinius.—Adults ($n = 7$). BRAZIL: AMAZONAS: Vai-Quem-Quer, Rio Juruá. INPA-H 4896 (holotype), 4903, 4904, 4905, 4912 (paratypes); Jaiú, Rio Juruá. INPA-H 3381, 3413 (paratypes).